TECHNICAL REPORT
NATICK/TR-15/027

AD _____

AN EVALUATION OF THE COMPRESSIVE PROPERTIES OF HELMET PADS PRE- AND POST-SHOCK WAVE OVERPRESSURE EXPOSURE

by
Marina Carboni
Xiaolin Zhen
Barry DeCristofano
and
Michael Maffeo

August 2015

Final Report
July 2012 – October 2013

U.S. Army Natick Soldier Research, Development and Engineering Center
Natick, Massachusetts 01760-5000

DISCLAIMERS

The findings contained in this report are not to be construed as an official Department of the Army position unless so designated by other authorized documents.

Citation of trade names in this report does not constitute an official endorsement or approval of the use of such items.

DESTRUCTION NOTICE

For Classified Documents:

Follow the procedures in DoD 5200.22-M, Industrial Security Manual, Section II-19 or DoD 5200.1-R, Information Security Program Regulation, Chapter IX.

For Unclassified/Limited Distribution Documents:

Destroy by any method that prevents disclosure of contents or reconstruction of the document.

REPORT DOCUMENTATION PAGE

Form Approved
OMB No. 0704-0188

1. REPORT DATE *(DD-MM-YYYY)*	2. REPORT TYPE	3. DATES COVERED *(From - To)*
14-08-2015	Final	July 2012-October 2013

4. TITLE AND SUBTITLE

AN EVALUATION OF THE COMPRESSIVE PROPERTIES OF HELMET PADS PRE- AND POST-SHOCK WAVE OVERPRESSURE EXPOSURE

5a. CONTRACT NUMBER

5b. GRANT NUMBER

5c. PROGRAM ELEMENT NUMBER

6. AUTHOR(S)

Marina Carboni, Xiaolin Zhen, Barry DeCristofano, and Michael Maffeo

5d. PROJECT NUMBER
13-103

5e. TASK NUMBER

5f. WORK UNIT NUMBER

7. PERFORMING ORGANIZATION NAME(S) AND ADDRESS(ES)
U.S. Army Natick Soldier Research, Development and Engineering Center
ATTN: RDNS-SEW-THB
Kansas St., Natick, MA 01760-5000

8. PERFORMING ORGANIZATION REPORT NUMBER
NATICK/TR-15/027

9. SPONSORING / MONITORING AGENCY NAME(S) AND ADDRESS(ES)

10. SPONSOR/MONITOR'S ACRONYM(S)

11. SPONSOR/MONITOR'S REPORT NUMBER(S)

12. DISTRIBUTION / AVAILABILITY STATEMENT
Approved for public release; distribution is unlimited

13. SUPPLEMENTARY NOTES

14. ABSTRACT

This report documents a study of the compressive properties between pre- and post-shock tube treated helmet pads under the on-going Headborne Equipment Shock Tube Methods Program in support of TeCD1b Force Protection-Soldier and Small Unit. The goal of this study was to determine whether the composite pad protection, designed for low velocity impacts in the Advanced Combat Helmet (ACH), exhibits measurable damage in compression performance after being loaded by an overpressure shock wave. Ultimately, this information will be used to determine whether the helmet pads can be re-used or if they need to be replaced after every exposure from a pressure loading in a shock tube or live fire blast. Rectangular and trapezoidal helmet pads were subjected to shock tube tests with the pads mounted inside a helmet set on a mannequin headform. The tests were conducted inside of a 28-inch x 28-inch shock tube with two overpressure durations and outside of a 9-inch x 9-inch shock tube at two distances from the exit of the tube for modified load profiles. The headform was oriented in four configurations with respect to the incoming shock: front facing, right side facing, back facing, and front facing at a 30^0 angle. The pads were removed from the helmet and subjected to either a dynamic impact drop tower assessment (305 cm/s) or a quasi-static compression test with an Instron materials test machine (8 mm/s). New helmet pads were subjected to the same compression tests, and the conditions of the two sets of pads were compared. No conclusions could be drawn from the drop tower assessment due to problems encountered with the data collection methods. No conclusive difference in compressive strength was observed from the quasi-static compression tests between the helmet pads subjected to an overpressure shock wave and the new pads.

15. SUBJECT TERMS

BLAST	DROP TESTS	BRAIN DAMAGE	VISCOELASTICITY
BRAIN	CONCUSSION	OVERPRESSURE	WOUNDS AND INJURIES
IMPACT	STATIC TESTS	PADS(CUSHIONS)	TEST AND EVALUATION
TRAUMA	HELMET PADS	HEAD(ANATOMY)	TRAUMATIC BRAIN INJURY
HELMETS	SHOCK TUBES	ACH(ADVANCED COMBAT HELMET)	

16. SECURITY CLASSIFICATION OF:			17. LIMITATION OF ABSTRACT	18. NUMBER OF PAGES	19a. NAME OF RESPONSIBLE PERSON Marina Carboni
a. REPORT	b. ABSTRACT	c. THIS PAGE			
U	U	U	SAR	40	19b. TELEPHONE NUMBER *(include area code)* 508-233-5461

This page intentionally left blank

Table of Contents

List of Figures

List of Tables

Acknowledgement

The authors would like to thank John Fitek for training with the drop tower impact method, Nick Tsantinis for help with troubleshooting the hardware trigger in the drop tower tests, and Jason Parker for the insights into helmet pad performance.

AN EVALUATION OF THE COMPRESSIVE PROPERTIES OF HELMET PADS PRE- AND POST-SHOCK WAVE OVERPRESSURE EXPOSURE

1. Introduction

This report documents a comprehensive study of the compressive performance and behavior of the Advanced Combat Helmet (ACH) impact protection pads before and after exposure to a blast wave. The goal of the analysis was to determine whether the helmet pads exhibited measurable damage in compressible performance when loaded by a shock overpressure. This work was performed by the Natick Soldier Research, Development and Engineering Center (NSRDEC), between July 2012 and October 2013, under the Headborne Equipment Shock Tube Methods Program in support of Technology Enabled Capability Demonstration (TeCD)1b Force Protection – Soldier and Small Unit. The overarching objective of the Headborne Equipment Shock Tube Methods Program is to determine the guidelines necessary for a repeatable shock tube laboratory test methodology for evaluating helmets and other headborne equipment under blast loading. Characterizing the response of the helmet pads to this environment and determining whether the pads should be replaced after every test is an important step in this analysis.

A series of experiments was performed to first expose the ACH pads to realistic overpressure conditions (e.g., internal and external to the tube) and then evaluate the change of compressive properties of post-shock wave exposure through both dynamic and quasi-static compression testing. Shock tubes at the University of Nebraska-Lincoln (UNL) were used to generate the overpressure conditions where helmet pads were mounted inside a helmet set on a mannequin headform. While the focus of this effort was only to measure the difference in compression between pre-test and post-test pads, the headform was instrumented with surface pressure sensors, three linear accelerometers, and three angular rate sensors to collect data for use in achieving the main program objective: establishing requirements for a laboratory test method for headborne equipment. The results of the pressure and acceleration data were analyzed and reported in a separate internal report: “Headborne Equipment Shock Tube Methods Development” [1].

Both a helmeted headform and a bare headform were placed inside a 28-inch x 28-inch shock tube for two different durations and outside a 9-inch x 9-inch shock tube at two different distances from the exit. The pads were evaluated based on two main criteria: their location inside of the helmet and with respect to their specific loading condition. In these test configurations, the incident blast overpressure varied from 172 to 241 kPa.

After exposure to the various shock profiles two methods were utilized to assess the compressive strength of the helmet pads: a dynamic impact test method (305 cm/s) using a drop tower [2] [3] and a quasi-static test (8 mm/s) using an Instron materials test machine. Though the much faster loading rate of the drop tower method makes it the preferred method for these measurements, the quasi-static data was sought for comparative purposes because the Instron machine provides a more controlled environment than the drop tower to assess the pads. Compressive stress and

strain data from both tests were used to calculate the maximum compression and total energy absorbed by the blast-exposed pads. Statistical analysis was performed where appropriate.

Chapter 2 of this report describes the ACH pads that were exposed to the shock tubes and how they were measured, the headform and instrumentation used in the shock tube treatments, the shock tube methodologies used, and the drop tower and Instron machine test setups and methodologies. Chapter 3 presents and discusses the results from both the dynamic drop tower and the quasi-static Instron machine compression tests. Chapter 4 discusses the conclusions drawn from the results of the compression tests.

2. Materials and Methods

2.1 ACH Pads

The ACH utilizes a Zorbium Action Pad (ZAP™) system for impact protection and as comfort liners. The ACH padding system consists of seven pads in three different shapes: four rectangular pads, two trapezoidal pads, and one circular crown pad. Figure 1 shows an arrangement of foam pads inside an ACH. The pads are polyurethane-based foam materials that exhibit rate-dependent stress-strain behavior. The pads absorb energy as they are compressed during an impact to the outer helmet shell. Gibson and Ashby [4] provide an extensive explanation of the energy absorbing capabilities of foam materials.

Figure 1. Proper arrangement of foam pads in ACH suspension system.

In this study, the helmet pads were categorized by their placement inside the helmet and on the headform: Front (Location F) and Back (Location B). The pads were in a composite structure of two layers of separate polyurethane foams enclosed in a plastic wrap, as shown in Figure 2. Outside of the plastic wrap there is a thin layer of additional padding on the bottom. The test specimens in this study were the full helmet pads, with no prior cutting preparations because removing the plastic wrap could affect the total pad system response [5].

Figure 2. Double-layered polyurethane foam pads wrapped in plastic.

The standard thickness of a pad as reported by the manufacturer is 19.05 mm (0.75 in) [6]. For this study, the length (L), width (W) and thickness (Thk) of each pad were measured using a 6-inch dial caliper (Mitutoyo Corporation, Model #: CD-S6"CT). Note that the pads did not have a uniform thickness; the central region of the pad was thicker than it was along the edges. In this study, the thicknesses were measured in the center region. Measuring foams precisely can be difficult and is often quite variable due to the compressibility of the foam. Since the helmet pads are soft, two metal plates with a thickness of 1.07 mm each were placed on the top and bottom of the pad to capture the thickness at the center of the pad. The recorded thickness measurements do not include the thicknesses of the two metal plates. In this study, only the trapezoidal and rectangular pads (not the circular pad) were evaluated because they received the strongest loading from the shock tube tests. Typical measurements for rectangular and trapezoidal pads are shown in Figure 3 and Figure 4, respectively.

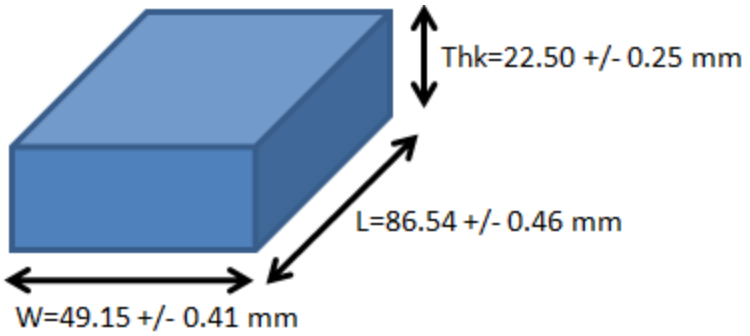

Figure 3. Typical measurements for a rectangular pad.

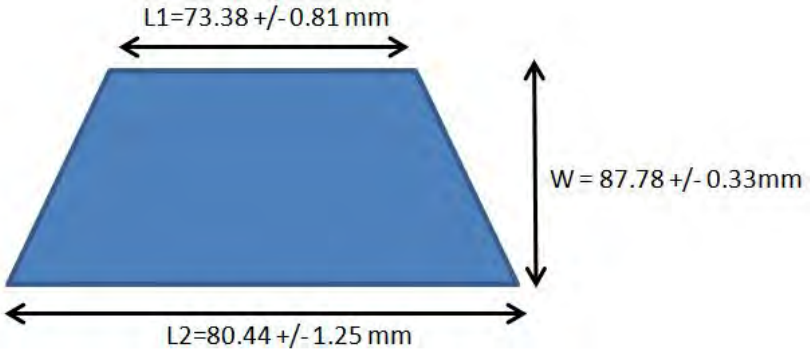

Figure 4. Typical measurements for a trapezoidal pad.

2.2 Headform and Instrumentation

The headform used in the shock tube was the Realistic Explosive Dummy (RED) Head (Figure 5). The University of Nebraska-Lincoln (UNL) worked with Humanetics to fabricate the RED Head, which is a simplified version of the Facial and Ocular Countermeasure for Safety (FOCUS) headform. The FOCUS headform is commercially available through Humanetics and was designed by them in collaboration with the Virginia Polytechnic Institute. The RED Head was designed to have the same surface geometry as the FOCUS when the rubber skin is included, but it does not include any of the force sensors in the face. The facial anthropometry of the FOCUS is based on a US Army Aeromedical Research Lab headform, which is stated to represent the 50th percentile male Soldier across the Army, Navy, and Air Force [7]. Based on

NSRDEC's test plan, the RED Head was modified to house 11 PCB 102B06 pressure sensors, from Piezotronics, Inc., which were mounted to the head and flush with the outer surface. Sensors 1-5 were located on the sagittal plane of the headform, while Sensors 6-8 and 9-11 were distributed on the sides of the headform. Sensors 1, 5, 7, and 10 (highlighted in orange in Figure 6) were the only uncovered surface pressure sensors when the helmet was on the headform. Three linear accelerometers (Endevco 7270a-6kg) and one angular rate sensor (DTS ARS PRO-18k) were placed at the CG of the RED Head. The outer skin of the head was removed so that the helmet pads interfaced with the hard polymeric surface of the headform (weight = 4.5 kg). This was done to ensure no false interaction of the rubber skin with the surface pressure sensors. Without the outer skin, the RED Head did not have ears or a well-formed nose. The headform was attached to a Hybrid III 50th percentile neck during the shock tube treatments. The initial results of the pressure and acceleration data were analyzed and documented in [1].

Figure 5. RED Head, manufactured by Humanetics and modified by UNL.

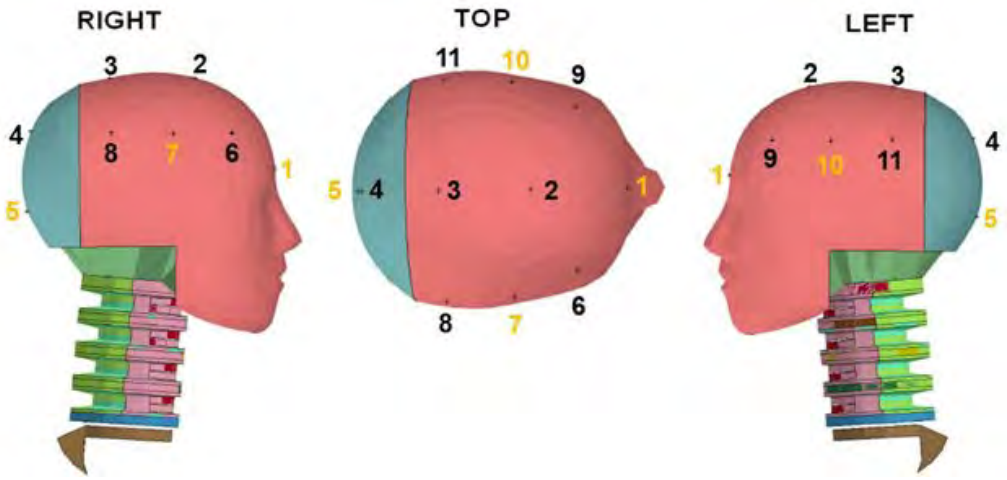

Figure 6. Surface pressure sensor locations on the RED Head.

2.3 Shock Tube Treatments

The test plan for the shock tube treatments, which included both internal and external shock tube testing, was designed by NSRDEC, and the experiments were performed in the Blast Simulation Laboratory at UNL. The purpose of testing internal and external to a shock tube was to evaluate the headform response in both test conditions with respect to a live-fire, free-field blast event. Measuring headform performance in the different conditions is important because the flow dynamics (static and dynamic pressure components) internal and external to a shock tube are typically not similar, even if the total pressure measurement is the same. This is due to the effects of the venting-jet flow generated when the shock exits the open end of the tube. Ritzel [8, 9] noted that, as the shock exits the tube, the dynamic pressure sometimes exceeds, by an order of magnitude, its proper proportion to the static (side-on) pressure. Therefore, these experiments were conducted in both test environments to collect data on headform response and to determine where the headform should be placed for the final laboratory test methodology recommendations, either internal or external to a shock tube.

In each shock tube, the treatments were conducted with both a bare headform (i.e., no helmet), and a helmeted headform in the following orientations: 1) front-facing the shock, head mounted at 0°, 2) front-facing the shock, head mounted 30° off axis, 3) side-facing the shock at 0°, and 4) back facing the shock at 0°. A front-facing 0° orientation was when the face was centered to the incoming shock wave with the pressure wave normal to and traveling directly towards the center of the face. A 30° orientation was when the head was tilted back 30° so that the chin was lifted up to the incoming pressure wave. The 30° rotation mimics when an explosion has been detonated in front of but below the face. Only helmet pads from the front facing and back facing test conditions were used in the compression tests because they were loaded in a more uniform and direct manner with respect to the incoming pressure wave.

The external shock tube treatments were conducted at a short distance (D1, which was 300 mm for the front facing orientation and 281 mm for the back facing orientation) and a longer distance (D2, which was 427 mm for the front facing orientation and 410 mm for the back facing orientation) from the exit opening of the 9-inch x 9-inch square shock tube. Figure 7 depicts the position of the RED Head in the front-facing 0° D1 scenario. Figure 8 is a schematic of the RED Head mounting locations for the front-facing and back-facing configurations with respect to the shock tube exit.

Figure 7. External shock tube exit with RED Head front facing at 0° and D1 [10].

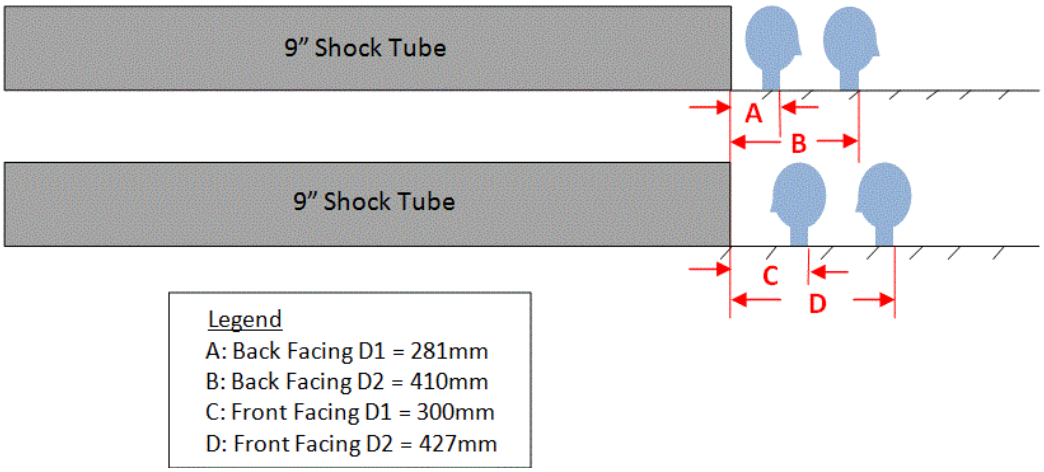

Figure 8. Location of RED Head mounting bases for external shock tube treatments at both D1 and D2 for front-facing 0° and back-facing 0° configurations.

The internal shock tube treatments were performed inside the 28-inch x 28-inch shock tube, at two positive overpressure durations: 2.5 ms (short duration) and 4 ms (long duration). Figure 9 is a schematic of the 28-inch x 28-inch shock tube system, as well as the locations of the RED Head and incident pressure measurements with respect to the location of the shock tube diaphragms.

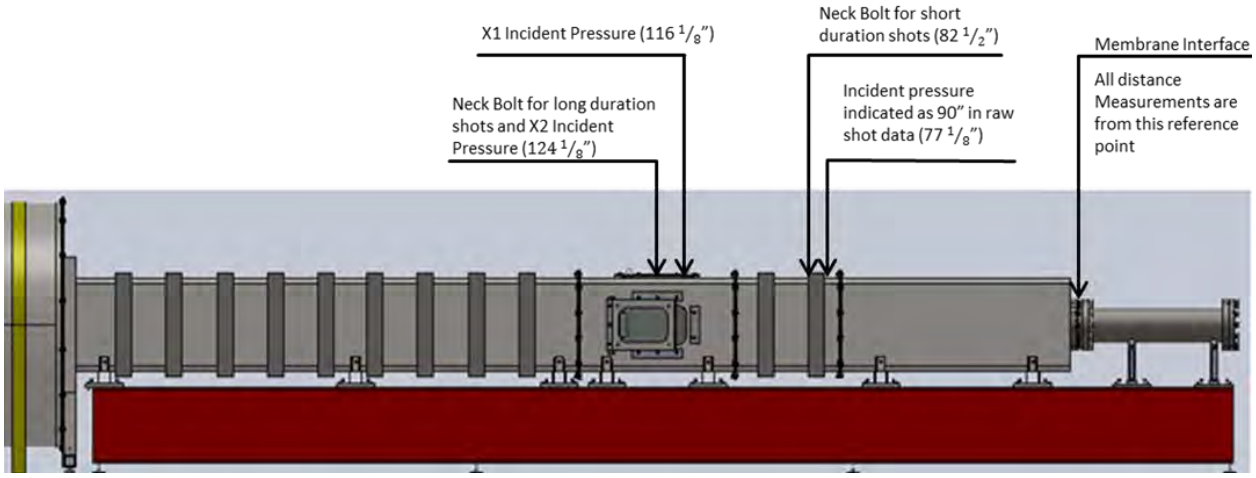

Figure 9. Location of RED Head and incident pressure measurements with respect to rupturing membranes[7].

The incident blast overpressure for the treatments in both shock tubes varied from 172 to 241 kPa (25 to 35 psi). The typical set of pressure-time traces for different test environments (i.e., free-field, internal shock tube, and external shock tube) are displayed in Figure 10. The average incident pressure is 170 kPa for the free-field profile, about 190 kPa for the 2.5-ms duration 28-inch shock tube treatments and 215 kPa for the 4-ms duration 28-inch shock tube treatments. However, the pressures provided for the 9-inch shock tube treatments (average of 230 kPa) were measured directly at the exit of the tube and not at the headform. Since the pressure drops off quickly once the shock wave exits the tube, the actual incident pressure was less than 230 kPa, but the exact value is not known. Additional testing is needed to obtain this measurement. As shown in Table 1, each shock tube configuration had four to six blasts with the helmet and four to eight blasts on the bare headform.

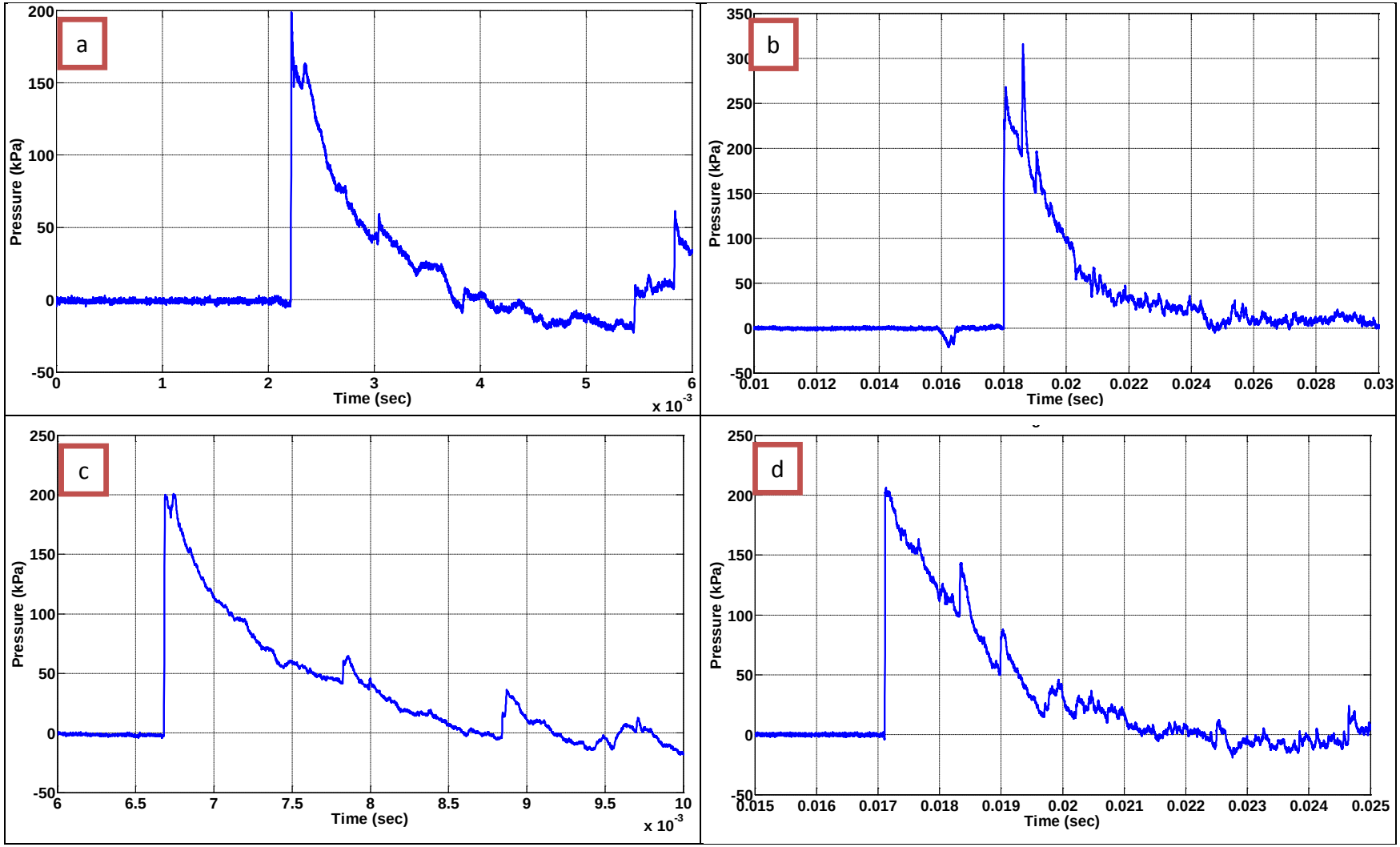

Figure 10.Typical set of pressure-time traces: (a) Free-field, (b) 9-inch shock tube at D1, (c) 28-inch shock tube for 2.5 ms, (d) 28 in shock tube at 4 ms.

Table 1. Number of overpressure tests by shock tube, headform orientation, and duration/distance.

Headform	28-Inch Internal Shock Tube Tested Pads				9-Inch External Shock Tube Tested Pads			
	Front Facing		Back Facing		Front Facing		Back Facing	
	2.5ms	4ms	2.5ms	4ms	D1	D2	D1	D2
Helmeted	5	4	4	4	6	5	5	5
Bare	8	4	6	4	4	4	5	5

2.4 Compression Tests

The drop tower impact dynamic compression tests and the Instron quasi-static tests were performed to evaluate the compressive properties of the ZAPs™ pre- and post-exposure to incident pressures of 172-241 kPa (25-35 psi) in several shock tube test configurations. As previously stated, the specimens were the fully intact helmet foam pads, with no prior cutting preparations. Table 2 provides the details of the drop tower and Instron tests that were performed on the post-shock tube treated helmet pads.

Table 2. Number of helmet pads tested in both compression tests by shock tube, headform orientation, duration/distance, and pad location in helmet.

Pad Shape	28-Inch Internal Shock Tube Tested Pads								9-Inch External Shock Tube Tested Pads							
	Front Facing				Back Facing				Front Facing				Back Facing			
	2.5ms		4ms		2.5ms		4ms		D1		D2		D1		D2	
	F	B	F	B	F	B	F	B	F	B	F	B	F	B	F	B
Drop Tower Test																
Rectangular	7	*	9	6	*	*	*	*	*	*	Untested		*	12	Untested	
Trapezoidal	4	*	5	4	*	*	*	*	*	*			*	5		
Instron Test																
Rectangular	*	10	*	*	*	*	10	10	10	10	Untested		10	*	Untested	
Trapezoidal	*	5	*	*	◯	◯	5	5	5	5			5	*		

F = Front pad location; B = Back pad location

* No pads were material tested in this condition. Pads from a given shock overpressure were only tested with either the drop tower or the Instron test method due to the limited number of pads from each test.

◯ Front pad location was preliminary quasi-static (Instron) tested under a different load cell (30 kN) with a 20 in/min crosshead speed; helmet pads were impacted to 8 mm/mm strain therefore these results are not included in this report.

2.4.1 Drop Tower Dynamic Impact Test

A description of the drop tower test method for evaluating foam materials is provided in [2]. That test method was adapted for material testing at NSRDEC. The drop tower test setup is shown in Figure 11 and Figure 12. In this study, the drop tower impact tests were conducted with a steel striker from a drop height of 500 mm measured from the surface of the helmet pad. The simplified striker geometry allows the impact attenuation of the pads to be directly compared, isolating the material response and eliminating the complexities of the full helmet system [5]. At the 500 mm drop height, the theoretical velocity of the striker can reach about 305 cm/s (10 ft/s or 7200 in/min). A small modification was also made to the hardware trigger position and mounting for this test setup. The hardware trigger was repositioned to better synchronize the experiment and the video. During the test, the light gate traveled with the striker and impacted

the hardware trigger to begin data acquisition; the light gate then passed the photodetector to capture the experimental velocity before impact. The impact force was measured with a PCB load cell (yellow square in Figure 11 and Figure 12), and the acceleration data were measured using a Kistler accelerometer (blue square in Figure 11 and Figure 12). The specifications of the drop tower test setup are provided in Table 3, and the data acquisition and sensor information for the setup is provided in Table 4.

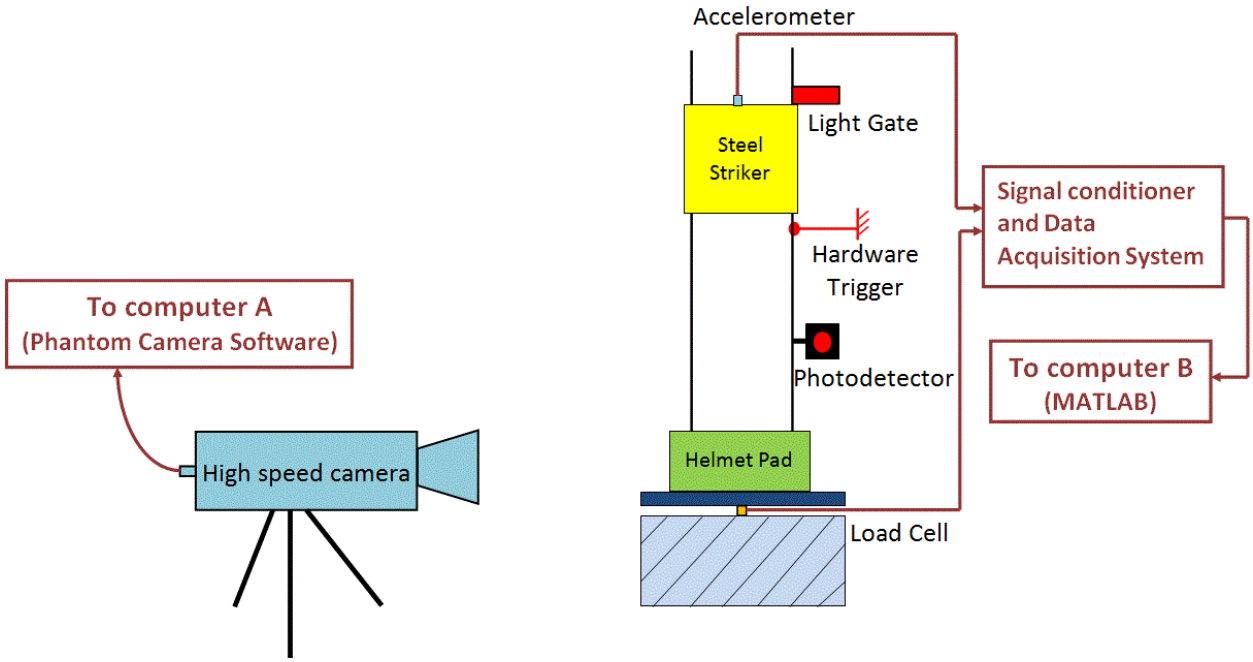

Figure 11. Schematic of drop tower test setup (right side view with respect to the camera).

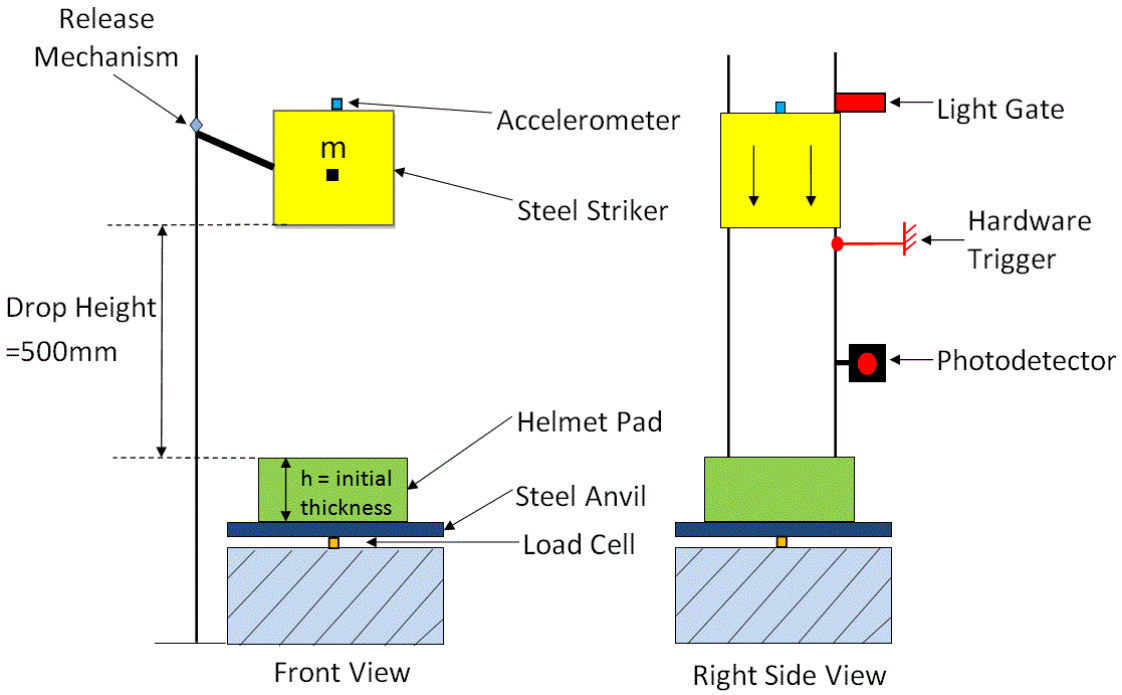

Figure 12. Front and right side views of drop tower setup with respect to the view of the high speed camera.

Table 3 Test specifications for the drop tower test setup.

Striker Material and Mass	Steel; 7.29kg
Striker Surface Area	0.0103 m^2 (16 in^2)
Drop Height	500mm measured from the top surface of helmet pad
Helmet Pad Specimen Area	Rectangular: 0.0042 ± 0.0002 m^2 Trapezoidal: 0.0067 ± 0.0001 m^2

Table 4 Data acquisition and sensor information for the drop tower test setup.

Data Acquisition System	National Instrument USB-6251/Matlab
Sampling Rate	10kHz
High Speed Video Camera Frame Size Frame Rate	Vision Research Phantom V710 512 x 512 10,000 frames/s
Accelerometer	Kistler 8704B500; sensitivity = 9.95 mV/g
Load Cell	PCB 200C20; sensitivity = 0.0543mV/N
Trigger	Hardware Trigger - Signal from contact switch simultaneously triggers data acquisition system and camera.

Multiple calculations of the stress and strain were compared to evaluate the accuracy of the results. Strain was calculated from the high speed camera and accelerometer data. Stress was calculated from the accelerometer and the load cell data. A brief description of the theoretical background for the drop tower method is provided in this section.

Assuming no energy loss in the drop mechanism, the potential energy (PE) of the striker mass at the drop height is equal to the kinetic energy (KE) of the striker at the foam surface, which in turn can be converted to the energy absorbed by the foam. As mentioned, data from both the accelerometer and the load cell were used to determine the stress (σ) on the foam independently. Equation 1 is used to calculate stress from the load cell data and Equation 2 is used to calculate stress from the accelerometer data; $\boldsymbol{F}$ is force, $\boldsymbol{a}$ is acceleration measured by the accelerometer, $\boldsymbol{A}$ is area of the impact surface and $\boldsymbol{m}$ is mass of the striker.

$$\sigma = F_{foam}/A_{foam} \quad (1)$$

$$\sigma = (m_{striker} \times a \times 9.81)/A_{foam} \quad (2)$$

In Equations 3 and 4, $\boldsymbol{\Delta v}$ is the change in velocity calculated from the accelerometer data, $\boldsymbol{\Delta x}$ is the compression of the foam, and $\boldsymbol{vi}$ is the initial steel striker velocity measured by the light gate timing and the known height of the light gate. The integration is performed from the first point of contact through impact. The time is verified by the high speed video.

$$\Delta v = \int a\, dt \quad (3)$$

$$\Delta x = \int (vi - \Delta v)\, dt \quad (4)$$

The strain in the foam (ε) is equal to the compression (Δx) divided by the initial thickness of the foam pad (h).

$$\varepsilon = \Delta x/h \quad (5)$$

In Figure 13, the acceleration measured by the accelerometer and the voltage output from the photodetector are plotted with respect to time. As expected, there is a drop in voltage when the light gate blocks the photodetector. The velocity before impact can then be calculated because the height of the light gate and the time of the voltage drop are known. The red arrows indicate the time required for the striker to travel the distance between the photodetector and the ZAP™ specimen. The high speed video is used to identify the first point in time that the striker impacts the test specimen. Knowing the start point is critical because it is used to integrate acceleration over time and calculate displacement and the strain in the helmet pad. In addition to the accelerometer measurement, the striker velocity and displacement are obtained from the high speed video, allowing for a second calculation of strain.

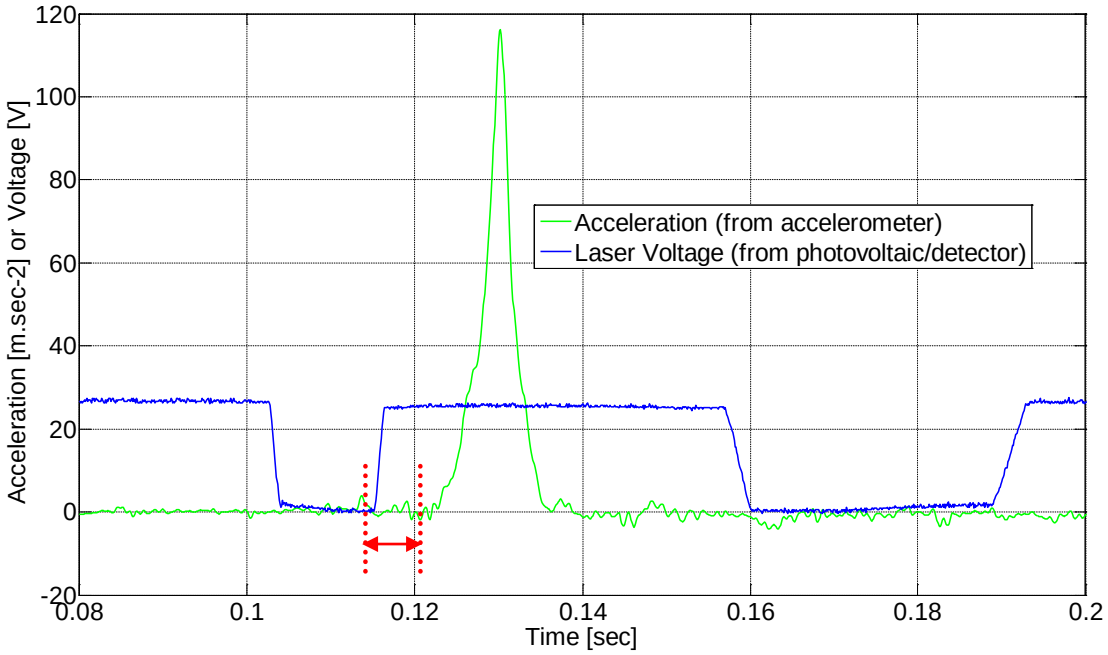

Figure 13. Superimposed time traces of the acceleration vs. laser voltage of a typical impact test.

2.4.2 Instron Quasi-Static Test

The quasi-static compression tests were conducted on a load frame Instron 4302 with a 10 kN load cell, located at NSRDEC. All tests were conducted at room temperature. The pad compression tests were performed with a crosshead speed of 8 mm/s (0.0278 ft/s or 20 in/min). These tests were performed up to 0.8 mm/mm strain. The helmet pads impact tested with the drop tower were not tested with the Instron because they were completely compressed and damaged during the drop tower impact. Using these pads for further evaluation would bias the results. Therefore, only pads that were shock tube tested and not evaluated with the drop tower were used for the quasi-static tests. As previously stated, the ZAPs™ do not have a uniform thickness; for each test specimen the measured thickness at the center of the pad was used to set the crosshead height to zero, as shown in Figure 14. Stress and strain values were recorded with the Bluehill® Materials Testing Software.

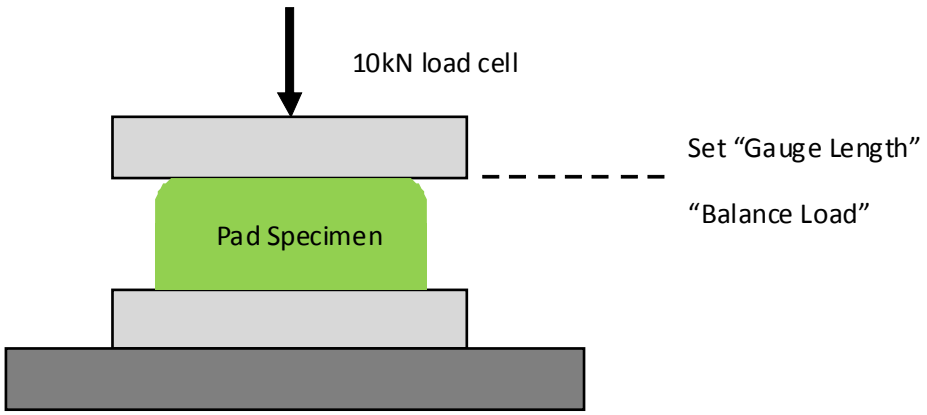

Figure 14. Instron test setup for the helmet pad compressive properties evaluation.

3 Compression Test Results and Discussion

The data collected from the drop tower tests and quasi-static compression tests are presented in this section. Stress, strain, and the absorbed energy were the primary metrics used in both drop tower dynamic impact tests and the Instron quasi-static tests to compare the new and shock-treated helmet pads. New pads have not been exposed to a shock overpressure. The compressive strength is reported with respect to the new and shock-tested pads with consideration for the pad shape (rectangular vs. trapezoidal), the blast test condition (front-facing vs. back-facing), and the pad locations within the helmet, front (F) or back (B). Statistical comparisons using independent sample t-tests were performed for the quasi-static compression tests only.

3.1 Drop Tower Dynamic Impact Test Results

Comparisons of the strain calculated from the high speed video and the accelerometer were performed. Some variation and errors were discovered with the use of the high speed video to calculate strain. The calculated impact velocities from the high speed video were within 10% of the theoretical velocity of 305 cm/s.

3.1.1 Image Results from Experimental Data

To either confirm experiment conditions or to calculate the stress and strain, four devices were used: 1) an accelerometer, 2) a load cell, 3) a photovoltaic detector, and 4) a high speed camera. Figure 15 and Figure 16 provide the experimental data reported from the load cell and the video data, respectively, from the drop tower tests. The stress-strain response of the helmet pad was analyzed as follows:

- Phase 1 (Point 1 → 2): Two plateau regions were observed, one for the softer foam (.1-.2 mm/mm strain) and one for the higher strength foam (0.45-0.6 mm/mm strain) .
- Phase 2 (Point 2 → 3): Densification region, up to around 0.87 mm/mm strain was observed.
- Phase 3 (Point 3 → 6): Rebound region was observed.

The trace up to Point 3 is the compression or loading region. After Point 3 is the unloading portion of the curve. The helmet pads were comprised of a viscoelastic material which exhibits a time-dependent response in returning to its original shape, as well as some energy lost during the impact. The dissipated energy is the difference between the loading and unloading cycles of the stress-strain curve.

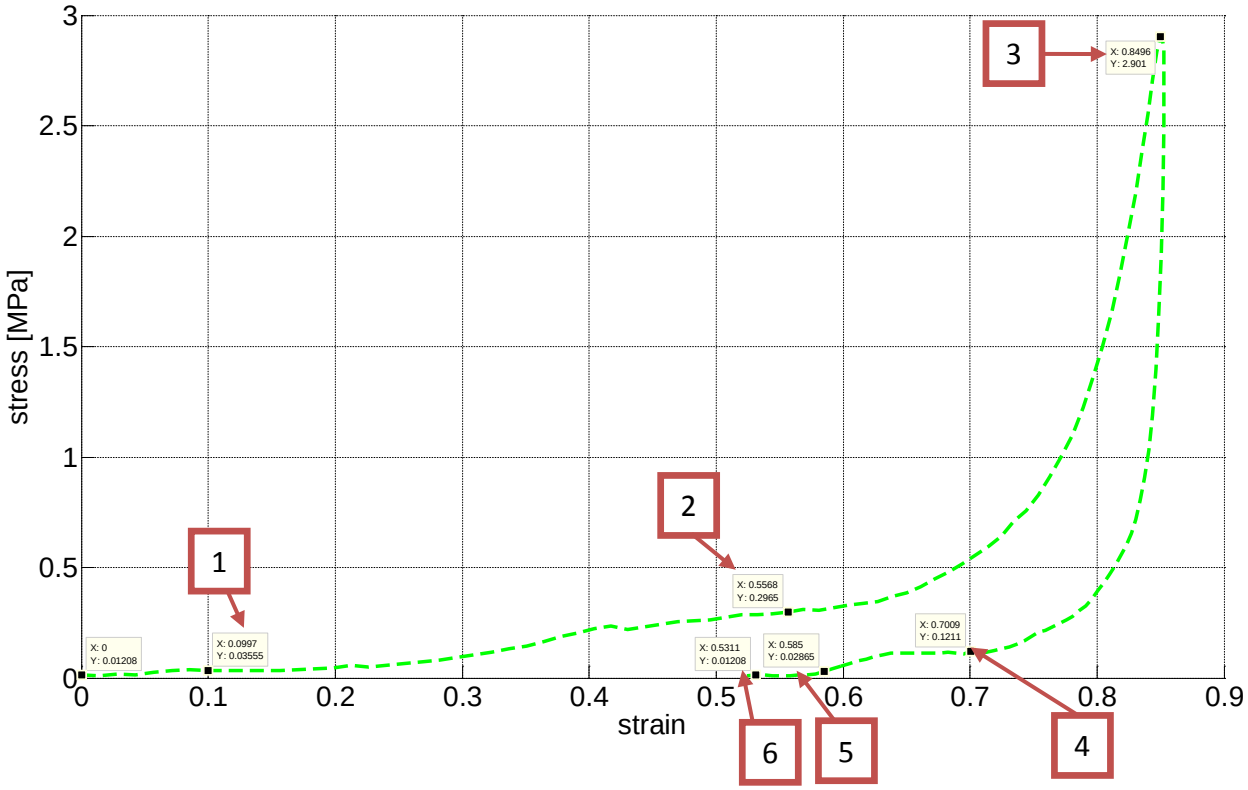

Figure 15. Stress vs. strain curve of a new pad impacted from drop tower test, with stress calculated from load cell data and strain calculated from accelerometer data.

Figure 16 is a series of six photos from the high speed video depicting a new pad being impacted in a drop tower test. The numbered frames correspond to the numbered transitional phases indicated in Figure 15. By t = 0.8 ms, the stress and strain remained in a linear relationship. At this point, the first plateau region was observed, from .1-.2 mm/mm strain. Then the stress increased until the second plateau region, 0.45 – 0.6 mm/mm strain, where Point 2 was at t = 3.7 ms. This is followed by the densification region where the stress quickly increased until the helmet pad was fully compressed. The maximum stress observed from the stress-strain curve was at t = 7.5 ms; it was followed by the relaxation region.

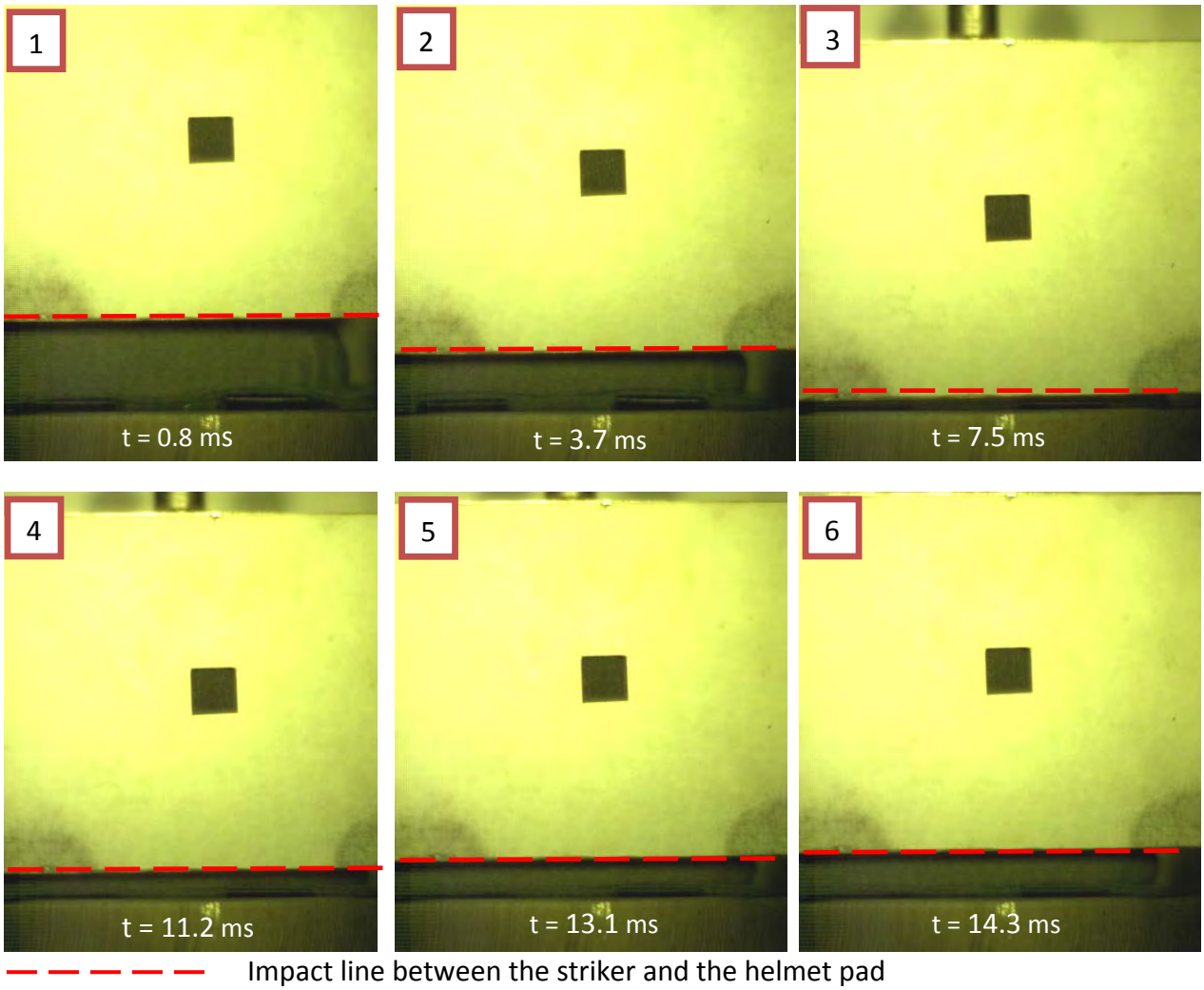

Figure 16. Series of images (10,000 frames/s) of the drop tower impact test on a new rectangular helmet pad.

3.1.2 Stress-Strain Curves

The data from the drop tower tests were evaluated in several ways. Preliminary data were first compared to those reported by Fitek [2] to ensure similar results were being obtained. Analysis was then performed to look at the stress-strain response based on the shape of the helmet pads, and the method used to calculate the strain (i.e., high speed video vs. accelerometer data) of the new vs. the shock-tested pads. For the stress measurement, the load cell generated the cleanest data, and therefore the stress results reported here are based on the load cell data. The strain was calculated using the high speed video and the accelerometer data. To clearly identify the shock tube treatment presented, a uniform naming convention was incorporated into the graphs in the following order: *shock tube test condition / headform orientation / helmet pad location*.

Figure 17 compares the preliminary trapezoidal data to those produced by Fitek. The strain in this figure was calculated using data from the accelerometer for the new pads and the high speed video from Fitek's data. In general, the data are similar, but with some differences. Fitek's data show that the pad entered the plateau region sooner, and it is sustained for slightly longer than the pad in the current study. The slopes of the densification region also differ slightly from each

other even, though the densification region began around the same strain, 0.6 mm/mm. The maximum stress shown in Fitek's data was 1.26 MPa when the strain was at 0.83 mm/mm, while the maximum stresses shown in the new pads from the current study were 0.99 ± 0.06 MPa when the strain was at 0.85 mm/mm. Overall, the results are similar, but with only one data point from Fitek's study, it is not possible to draw a conclusion on statistical significance.

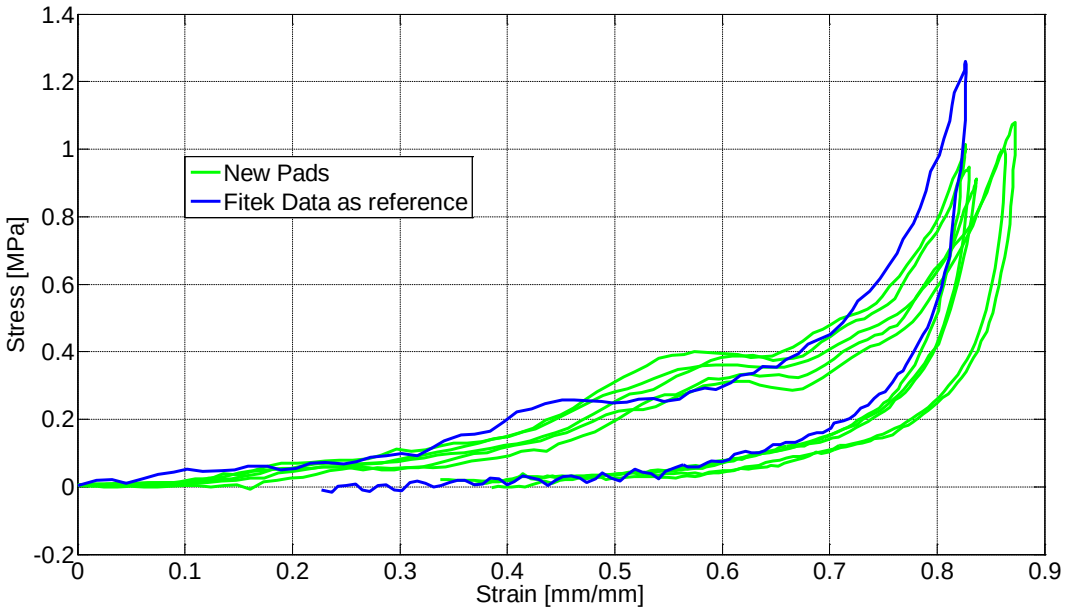

Figure 17. Preliminary drop tower dynamic test data for trapezoidal pads compared with Fitek's data.

Once satisfied the data mirrored Fitek's results, an analysis of the calculated strain was performed using both the high speed video and accelerometer data for the new pads (Figure 18). Fitek's preferred method was to calculate the stress from the load cell and the strain from the high speed video. However, using this method, the data from the current study had errors in the stress-strain curves, and a significant amount of variation was observed in the calculated strain. An example of an erroneous stress-strain curve can be found in Figure 18a, where there is a loop present. The authors determined there were several circumstances in the data collection methods which contributed to the errors in the calculated strain. The "loop" observed in Figure 18a was a result of noise in the high speed video due to a problem with the camera. This noise affected the image processing of the data used to calculate compression; the camera itself was ultimately fixed, but the data could not be improved. Additional variations in the data involve procedures that can be improved. For instance, user interpretation of the first contact point between the steel striker and test specimen is required in order to accurately calculate pad compression (i.e., measure strain from the high speed video and accelerometer). Therefore, user judgment is required to best select the first contact point to start the calculation. This was done by observation of the high speed video in comparison with the acceleration and load cell data. This method could be more precise, and future work is needed to improve this. Despite some of the errors encountered, there were several data sets which showed a good comparison between the video and the accelerometer. Figure 18b and Figure 18c display sample comparisons of these data.

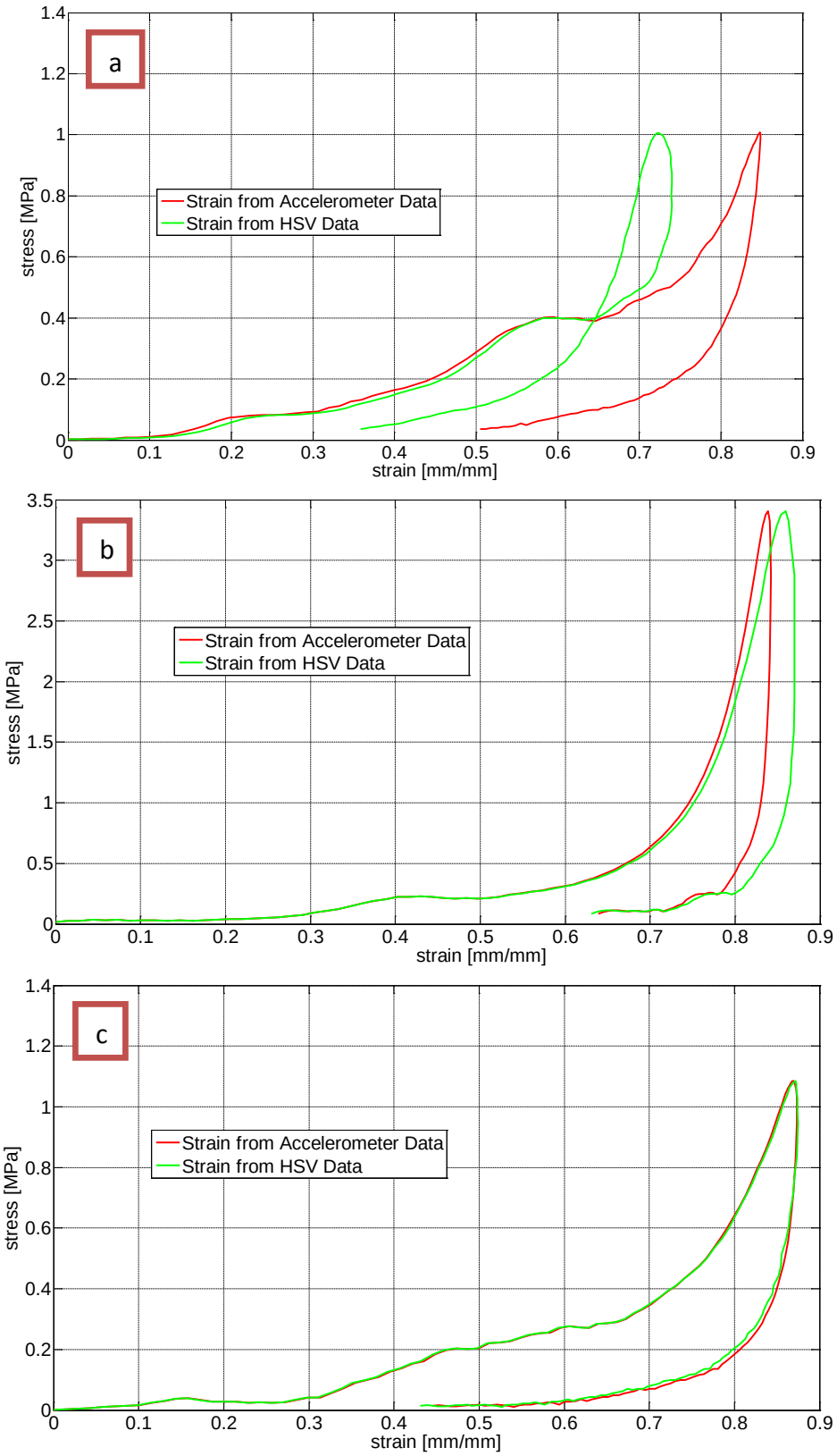

Figure 18. Typical dynamic stress-strain curve comparisons using strain from accelerometer and high speed video: (a) Erroneous results where the calculated strains do not match, (b) Slightly offset results in the unloading portion of the curve, (c) Nearly exact comparison of the calculated strain.

Using the authors' interpretation of the start point, the strain calculated from the accelerometer data had less variability than the strain from the high speed video. A comparison of a subset of the new and shock-tested helmet pads using the accelerometer data to calculate strain is provided in Figure 19. Figure 19a and Figure19b display the sample stress-strain results of rectangular and trapezoidal pads, respectively. From this data, no difference in compressive strength of the new and shock-tested pads was observed.

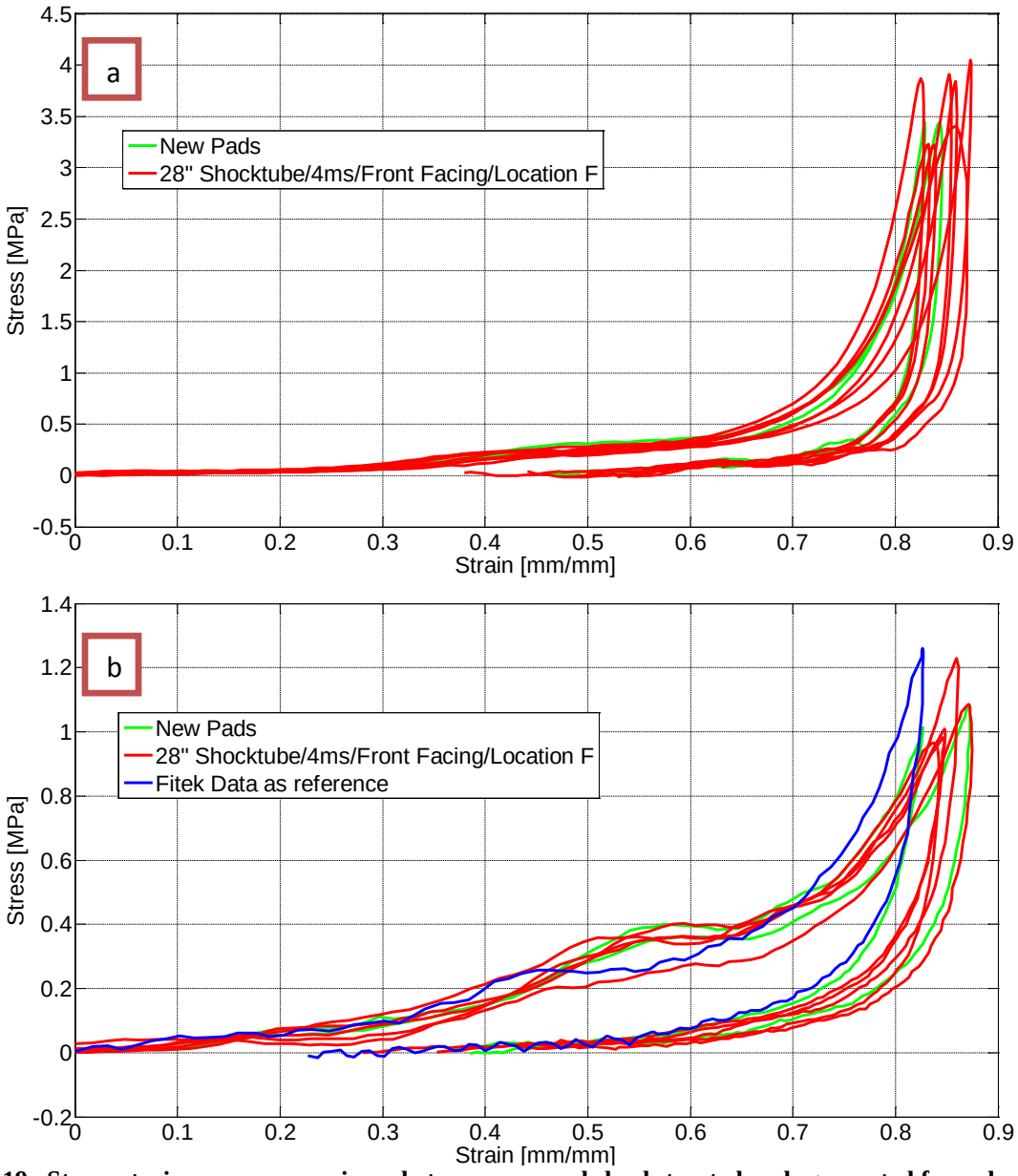

Figure 19. Stress-strain curve comparisons between new and shock-treated pads generated from drop tower test, strain calculated from accelerometer data: (a) Rectangular pads, (b) Trapezoidal pads.

The authors did observe a difference in response of the rectangular and trapezoidal shaped pads after 0.7 mm/mm strain. Figure 20 displays typical stress-strain curve comparisons between the rectangular and trapezoidal pads tested in a drop tower machine. All results were reported from new pads using the accelerometer-based strain. From the data, the maximum stress for a

rectangular pad was about 3.64 ± 0.36 MPa, and the maximum stress for a trapezoidal pad was about 1.02 ± 0.07 MPa. This means the maximum compressive stress for rectangular pads was more than double that of the trapezoidal pads. The average surface area for a trapezoidal pad was 0.0067 ± 0.0001 m^2, while the average surface area for a rectangular pad was 0.0042 ± 0.0002 m^2. As the pads were constructed of the same material, the observed differences were likely a function of non-uniform shape, edge effects, and helmet pad construction (i.e., variation in the seal provided of the plastic wrap). In order to continue evaluating the helmet pads and to better understand and improve the drop tower test method before conducting further tests with it, the authors decided to perform Instron quasi-static tests, which were not originally planned for this study, and focus on the results from those tests as the primary source of data for this study.

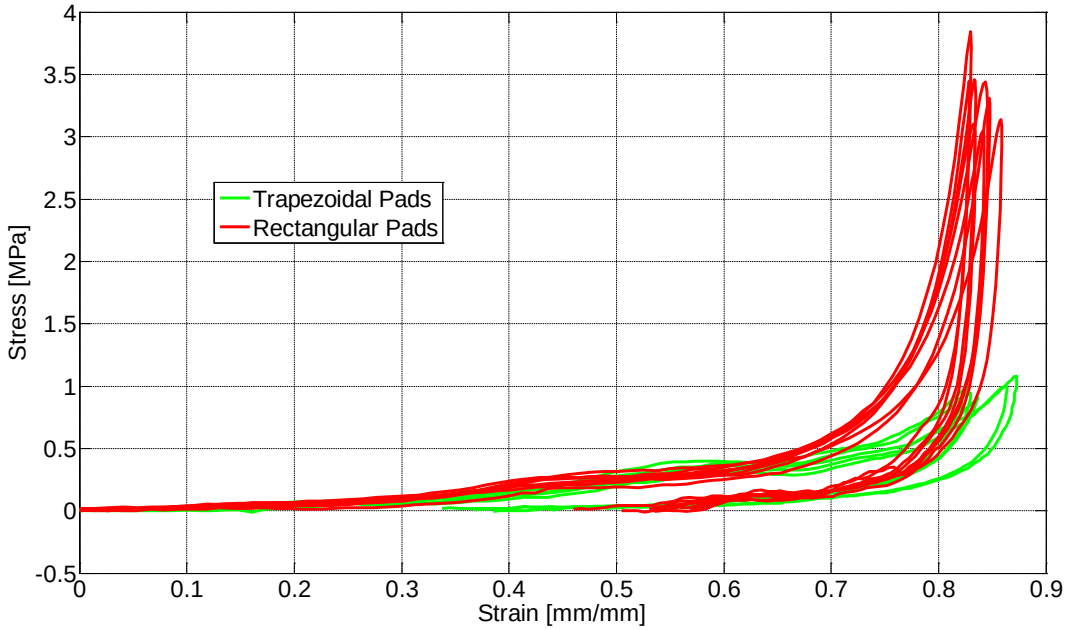

Figure 20. Stress vs. strain results for rectangular and trapezoidal pads from drop tower tests using strain calculated from accelerometer data.

3.2 Instron Quasi-Static Test Results

Stress-strain profiles from the Instron quasi-static tests for new pads overlap with those for blast tested pads. The stress at 0.8 mm/mm strain and the absorbed energy up to this strain were calculated from the experimental data. Evaluation of the data with respect to pad shape, test condition, and location of the helmet pad shows that only 2 of the 12 conditions showed statistically significant differences. However, statistical comparisons from the data pooled by pad shape and test condition resulted in no statistically significant differences between the new and shock-tested helmet pads.

3.2.1 Stress-Strain Curves

Figure 21, Figure 22, Figure 23, and Figure 24 show a sample of the stress-strain curves from pads tested outside the 9-inch shock tube at D1 and inside the 28-inch shock tube at 2.5 ms in comparison to the new pads. The stress-strain curve profiles appear to be similar for all tested scenarios. Additional stress-strain curves are summarized in Appendix A. Profiles of these new and blast-tested pads overlapped each other with no visible observable differences. The

variations were small in the linear elastic portion, which was up to 0.20-0.25 mm/mm of strain. The variation then gradually increases after the elastic limit. The densification region started at about 0.55-0.60 mm/mm strain for both new and blast-tested pads. Compressive forces required to act on the foams rapidly increased as strain increased.

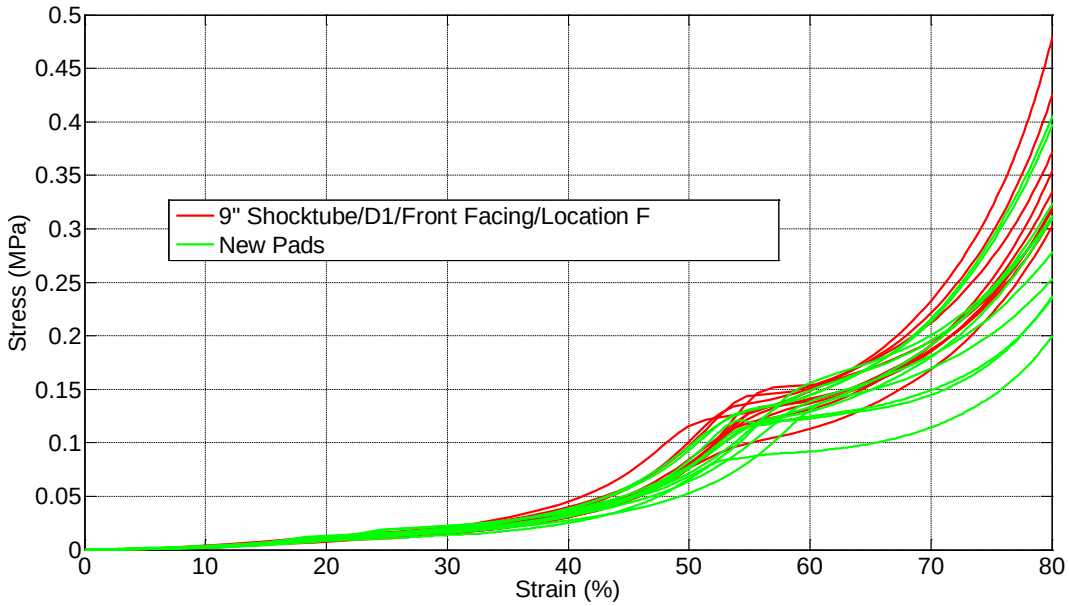

Figure 21. Quasi-static test stress-strain curves for rectangular pads treated outside 9-inch shock tube at D1and untreated.

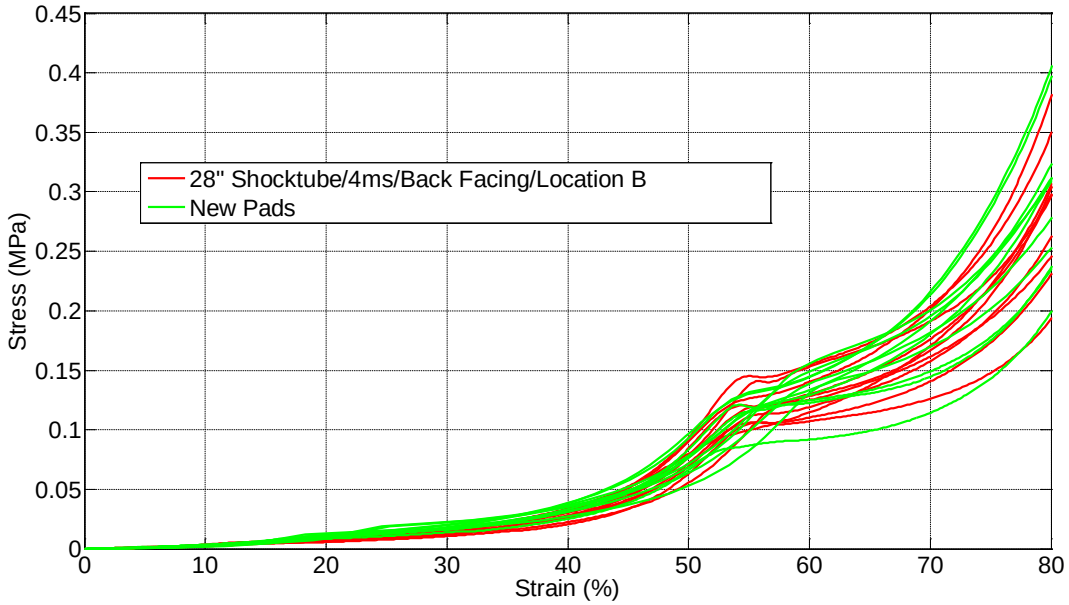

Figure 22. Quasi-static test stress-strain curves for rectangular pads treated in 28-inch shock tube at 4 ms and untreated.

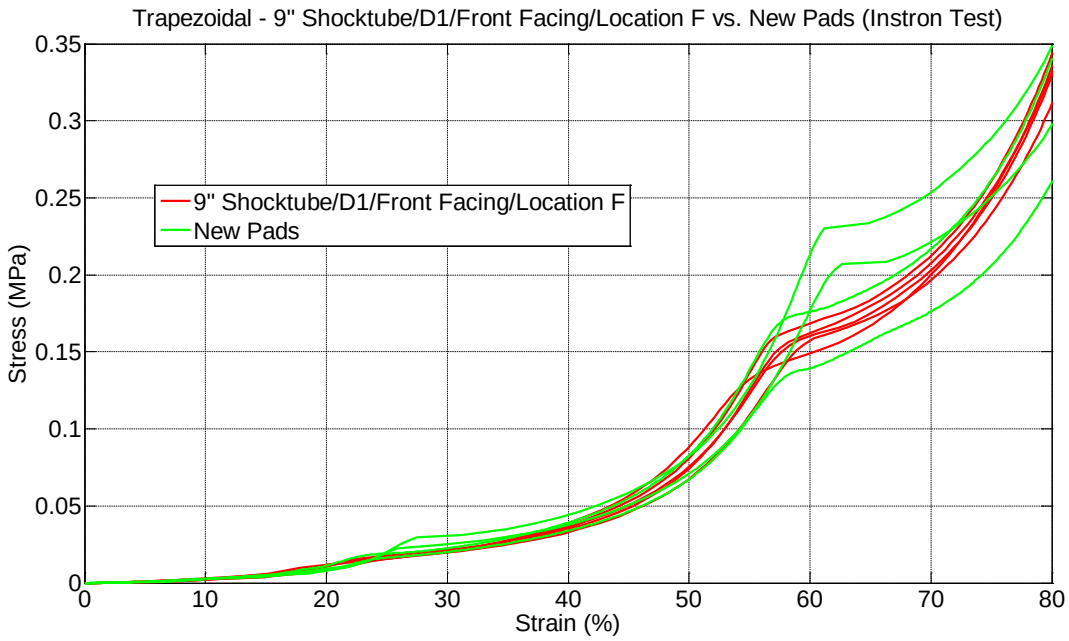

Figure 23. Quasi-static test stress-strain curves for trapezoidal pads outside 9-inch shock tube at D1and untreated.

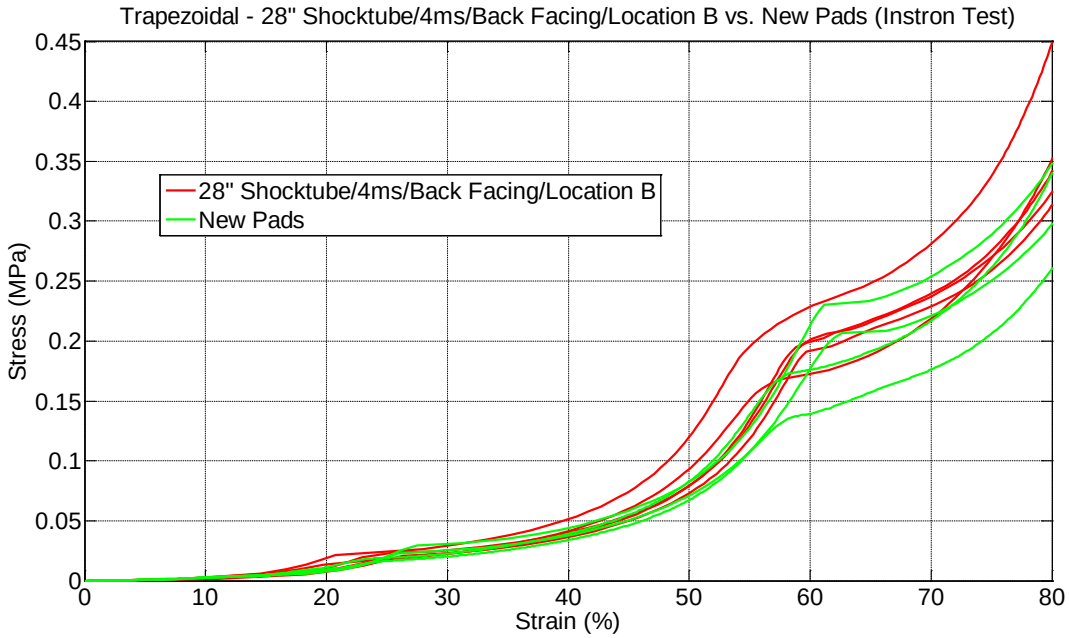

Figure 24. Quasi-static test stress-strain curves for trapezoidal pads treated in 28-inch shock tube at 4 ms and untreated.

3.2.2 Stress at 0.8 mm/mm of the Strain

The stresses at 0.8 mm/mm strain for the different test conditions and pad geometries were also compared. For the trapezoidal pads, the average stress required to compress new pads to 0.8 mm/mm strain was 0.32±0.045 MPa, while the stress required to compress shock tube treated pads was 0.33±0.04 MPa. For the rectangular pads, the average stress at 0.8 mm/mm strain was 0.30±0.065 MPa for new pads and 0.32±0.05 MPa for shock-tested pads. Figure 25 and Figure

26 compare the stress of new pads and shock-tested pads in different scenarios for trapezoidal pads and rectangular shaped pads, respectively.

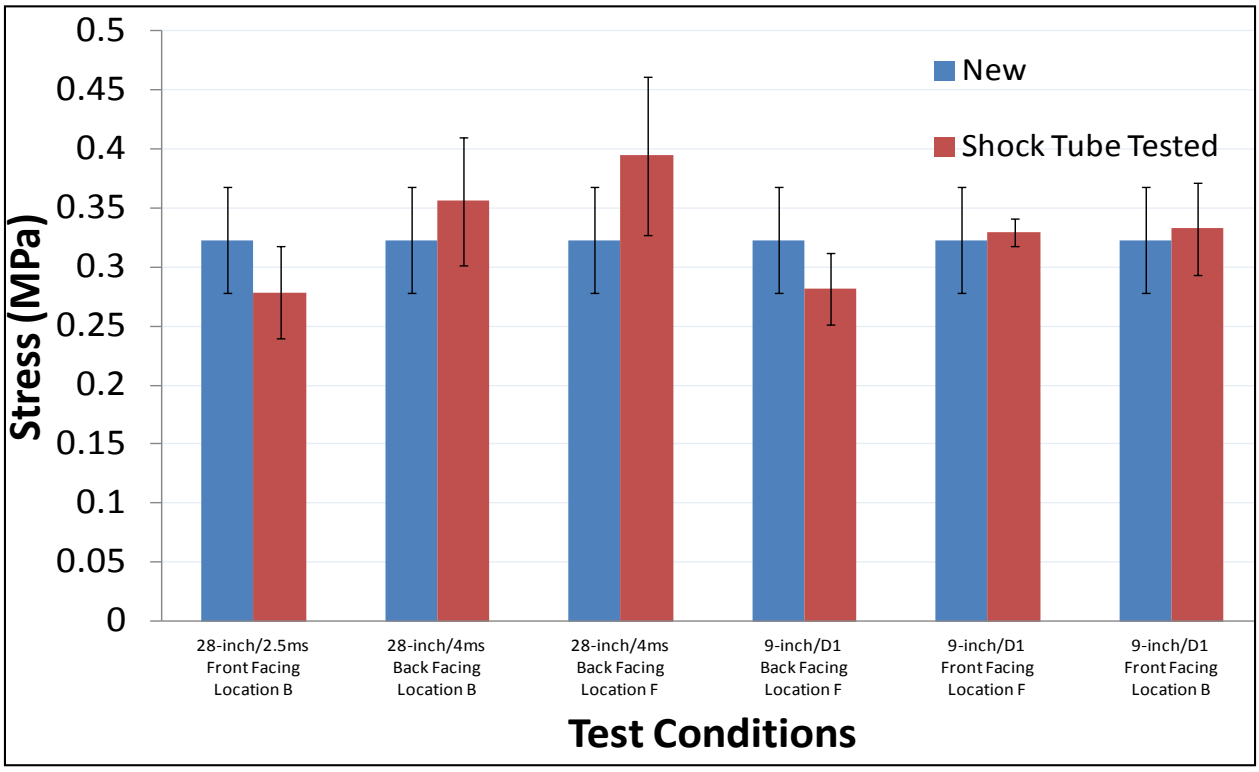

Figure 25. Quasi-static test stress at 0.8 mm/mm strain for trapezoidal pads shock tube treated and untreated.

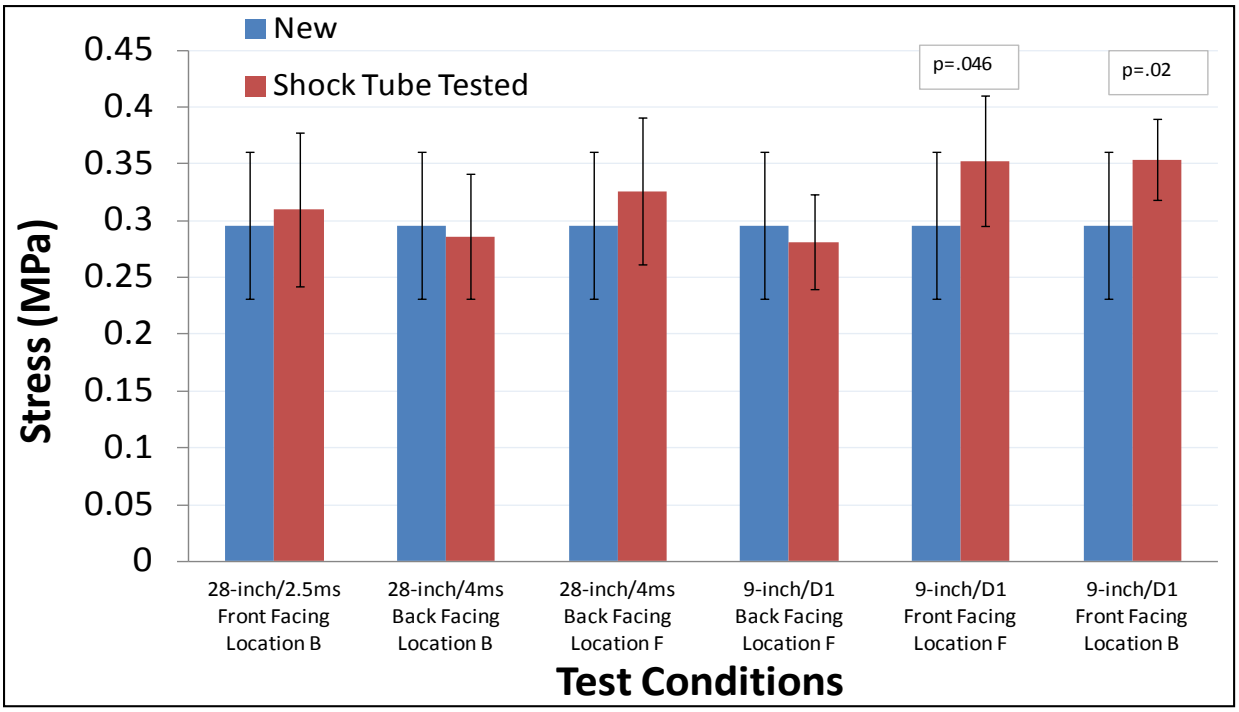

Figure 26. Quasi-static test stress at 0.8 mm/mm strain for rectangular pads shock treated and untreated.

Two-tailed independent sample t-tests were performed to statistically compare untreated and shock-treated pads. For the trapezoidal pads, there were no statistically significant differences between internal (28-inch) shock tube treated pads and new pads or between external (9-inch) shock tube tested pads vs. new pads. For the rectangular pads, statistically significant differences were observed in two of the 9-inch shock tube conditions (p=0.046, p=0.02, identified in Figure 26). However, no statistically significant differences were observed when data from all pads treated in the 9-inch shock tube were combined, regardless of pad shape and treatment condition, and compared with the new pads.

3.2.3 Energy up to 0.8 mm/mm of Strain

The absorbed energy (up to 0.8 mm/mm of strain) was also compared between the new pads and shock-treated pads. For the trapezoidal pads, the absorbed energy was 70.3±8.6 kPa-mm/mm in new pads and 70.4±7.8 kPa-mm/mm in shock-treated pads. For the rectangular pads, the absorbed energy was 58.4±8.9 kPa-mm/mm in new pads and 62.3±8.1 kPa-mm/mm in shock-treated pads. Figure 27 and Figure 28 compare the absorbed energy between the new and shock-treated pads in each condition for the trapezodial and rectangular pads, respectively.

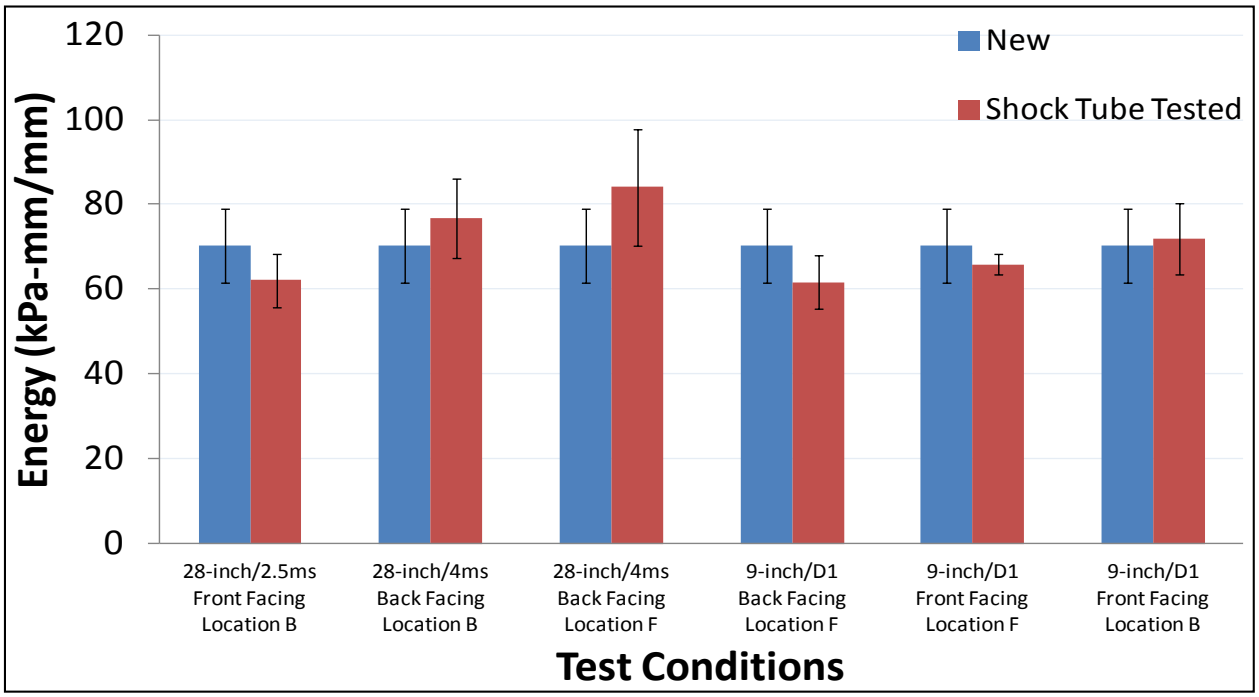

Figure 27. Quasi-static test absorbed energy in trapezoidal pads up to 0.8 mm/mm strain shock-treated and untreated.

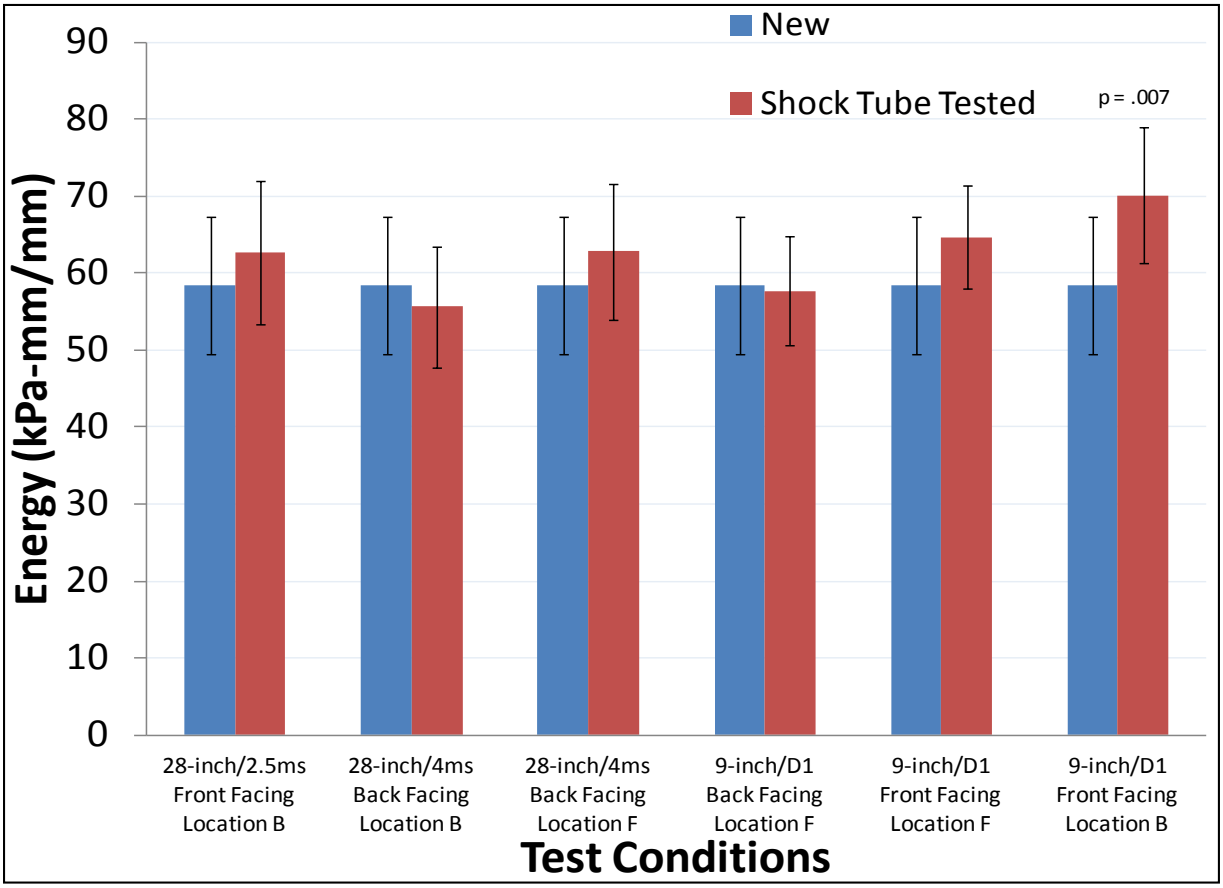

Figure 28. Quasi-static test absorbed energy in rectangular pads up to 0.8 mm/mm strain shock-treated and untreated.

Again, two-tailed independent sample t-tests were performed between new pads and shock-treated pads for the total absorbed energy results. There was no statistically significant difference between new pads and pads shock-treated in the 28-inch shock tube. Only one set of pads treated in the 9-inch shock tube was statistically different from the new pad results ($p=0.007$, shown in Figure 28). However, no statistically significant differences were observed when the absorbed energy in all the pads treated in the 9-inch shock tube was combined, regardless of pad shape and treatment condition, and compared with the absorbed energy in the new pads, .

4 Conclusions

The overall goal of this study was to determine if there is a significant difference in compressive strength between new and shock-treated ACH impact protective pads. ACH ZAPs^{tm} were first subjected to a series of shock tube treatments while mounted inside of an ACH on a headform. The rectangular and trapezoidal (but not the circular) ACH pads were assessed. Two test methods were then used to evaluate the compressive strength of the shock-treated pads: 1) a dynamic drop tower impact test and 2) a quasi-static test using an Instron materials test machine.

The drop tower impact compression test was initially the only test performed (and planned) because it has a much faster loading rate (305 cm/s) than the quasi-static compression test performed using an Instron materials test machine. However, due to some inconsistencies observed between the strain calculated from the high speed video and the acceleration measurements, quasi-static tests were used to complete the analysis. The authors attribute the variation in the calculated strain to the current test procedures, the non-uniform pad shape/size, and the plastic seal around the foam pads. One problem with the current drop tower test procedure involves user interpretation of the first contact point in order to accurately determine pad compression (i.e., measure strain) using the high speed video and accelerometer data. A possible improvement in the drop tower test would be to remove the need for user interpretation to complete the strain calculation. This can be achieved by including a contact circuit between the bottom of the striker and the helmet pad to directly measure the initial point of contact. This will ensure a consistent evaluation metric for each test specimen and is currently being implemented.

Quasi-static compression tests were conducted with an Instron materials test machine to improve the variation in the data. The results from the quasi-static tests were more consistent and the remaining helmet pads were assessed using this method. For statistical comparisons, when the data were evaluated with respect to pad shape, test condition, and location within the helmet pad for maximum stress it was found that only 2 of the 12 conditions showed statistically significant differences. Statistical comparisons from the data pooled based on pad shape and test condition resulted in no statistically significant differences between the new and shock-treated helmet pads. Similar results were found for the comparison of absorbed energy. However, this work was only part of an ongoing effort under the Headborne Equipment Shock Tube Methods Program, and ACH pads will continue to be assessed in order to fully characterize exposure to the various overpressure test conditions such as live fire free-field explosive tests and other loading conditions within the shock tube.

This document reports research undertaken at the U.S. Army Natick Soldier Research, Development and Engineering Center, Natick, MA, and has been assigned No. NATICK/TR- 15/027 in a series of reports approved for publication.

5 References

[1] M. Carboni, B. DeCristofano, M. Maffeo and J. Cyganik, "Headborne Equipment Shock Tube Methods Development Interim Report," US Army Natick Soldier RD&E Center Internal Report, 2014.

[2] J. Fitek, "Design of a Helmet Liner for Improved Low Velocity Impact Protection," US Army Natick Soldier RD&E Center TR-13-016, 2012.

[3] J. Fitek, "Testing and Modeling the Dynamic Response of Foam Materials for Blast Protection," University of Massachusetts, Lowell, 2010.

[4] L. J. Gibson and M. F. Ashby, Cellular Solids, Cambridge, UK: Cambridge University Press, 1997.

[5] W. C. Moss and M. J. King, "Impact response of US Army and National Football League helmet pad systems," Lawrence Livermore National Laboratory, 2011.

[6] "Team Wendy Materials," Team Wendy, [Online]. Available: http://www.teamwendy.com/technology/materials/..

[7] E. A. Kennedy, "The Development and Validation of a Biofidelic Synthetic Eye for the Facial and Ocular Countermeasure Safety (FCUS) Headform," Virginia Polytechnic Institute and State University, Blackburg, Virginia, 2007.

[8] Dyn-FX Counsulting Ltd., "Dyn-FX Technical Note TN050901: End-Jet Testing as Simulation of Explosion Blast Conditions".

[9] David V. Ritzel, Steve A. Parks, Jim, Roseveare, Gerry Rude, and Thomas W. Sawyer, "Experimental Blast Simulation for Injury Studies," NATO-OTAN.

[10] N. Chandra, "Experimental Evaluation of Measurement Methodology for Primary Blast Loading Conditions," Draft, 2013.

Appendix
Quasi-Static Tests Results

The results from the tests of the rectangular pads under 10 kN load cell (crosshead speed = 8 mm/s) are displayed in Figures A-1 through A-6.

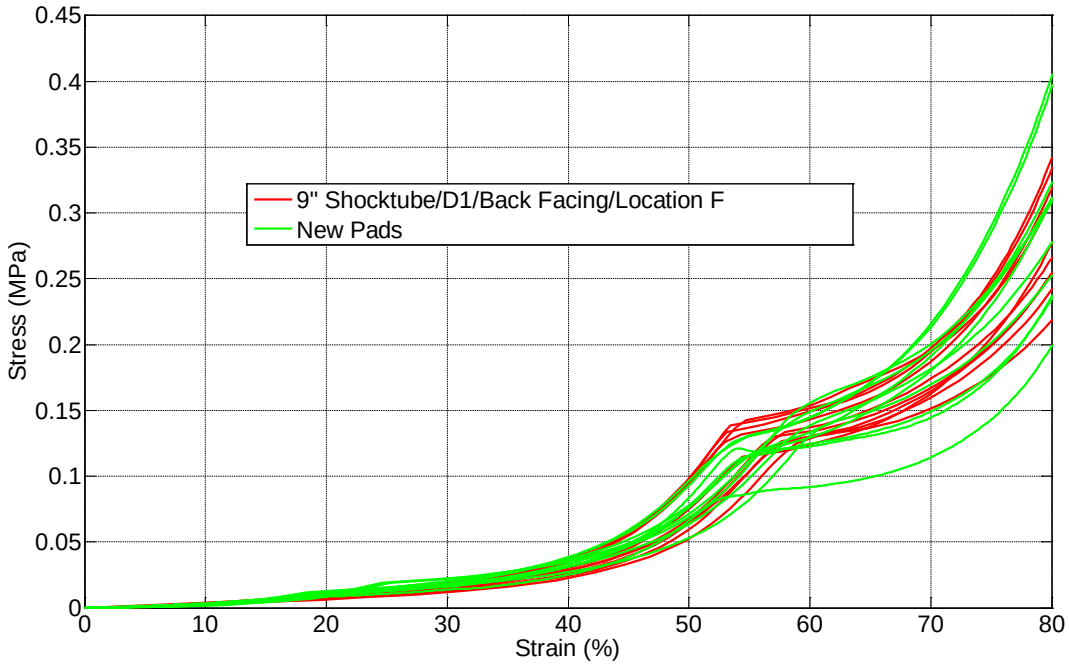

Figure A-1. Rectangular-9-inch shocktube/D1/back facing/location F vs. new pads.

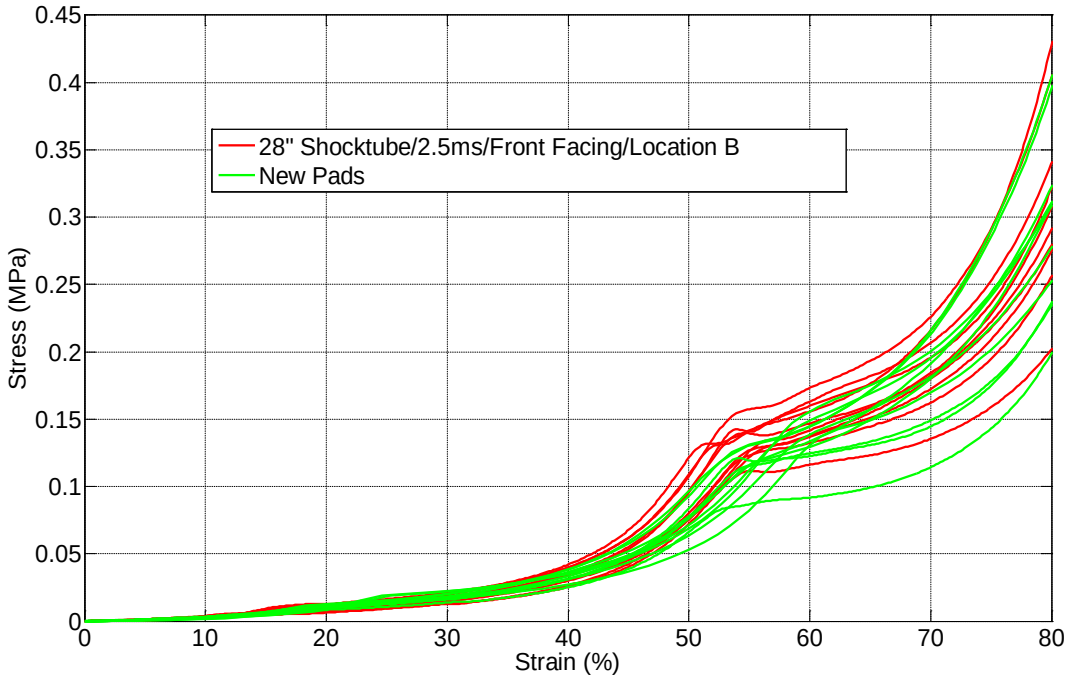

Figure A-2. Rectangular-28-inch shocktube/2.5-ms/front facing/location B vs. new pads.

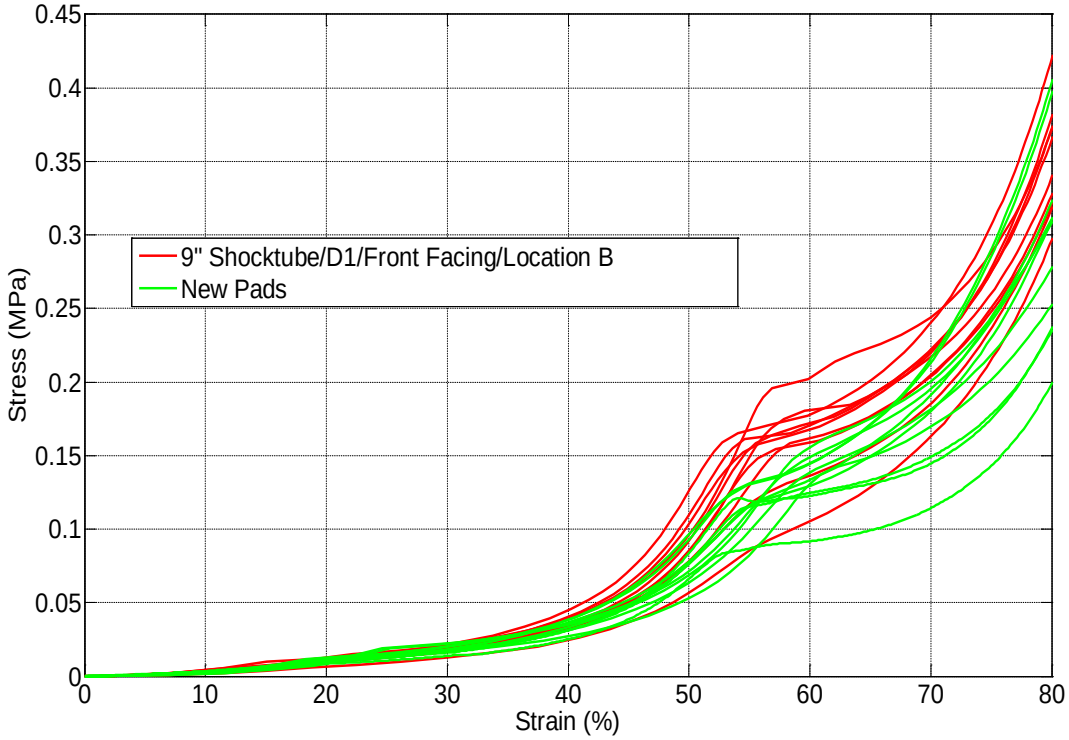

Figure A-3. Rectangular-9-inch shocktube/D1/front facing/location B vs. new pads.

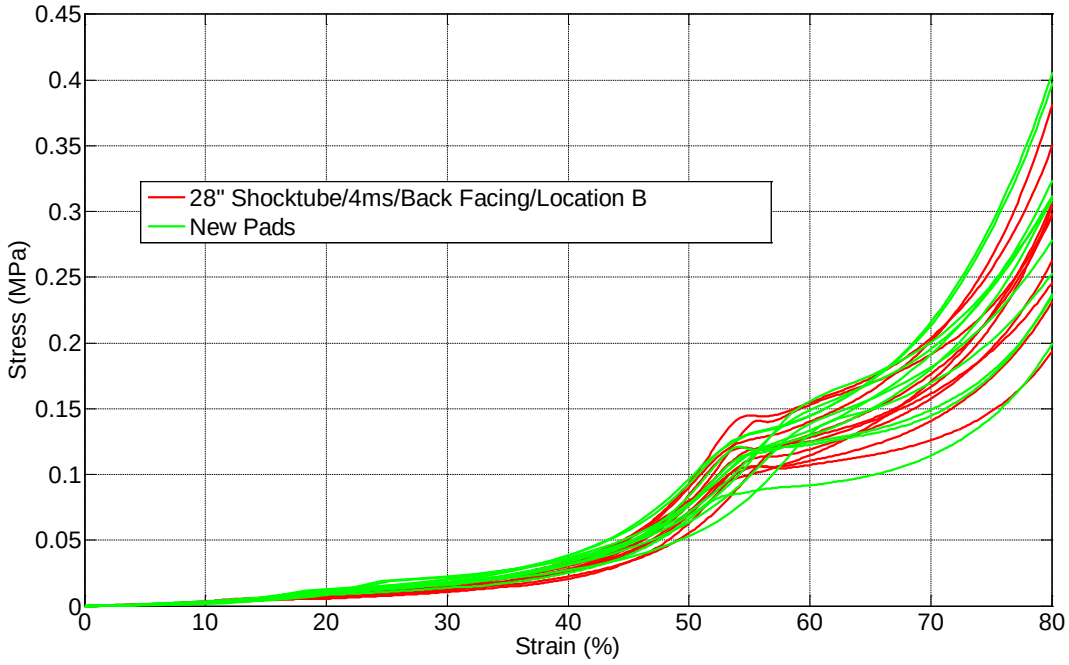

Figure A-4. Rectangular-28-inch shocktube/4-ms/back facing/location B vs. new pads.

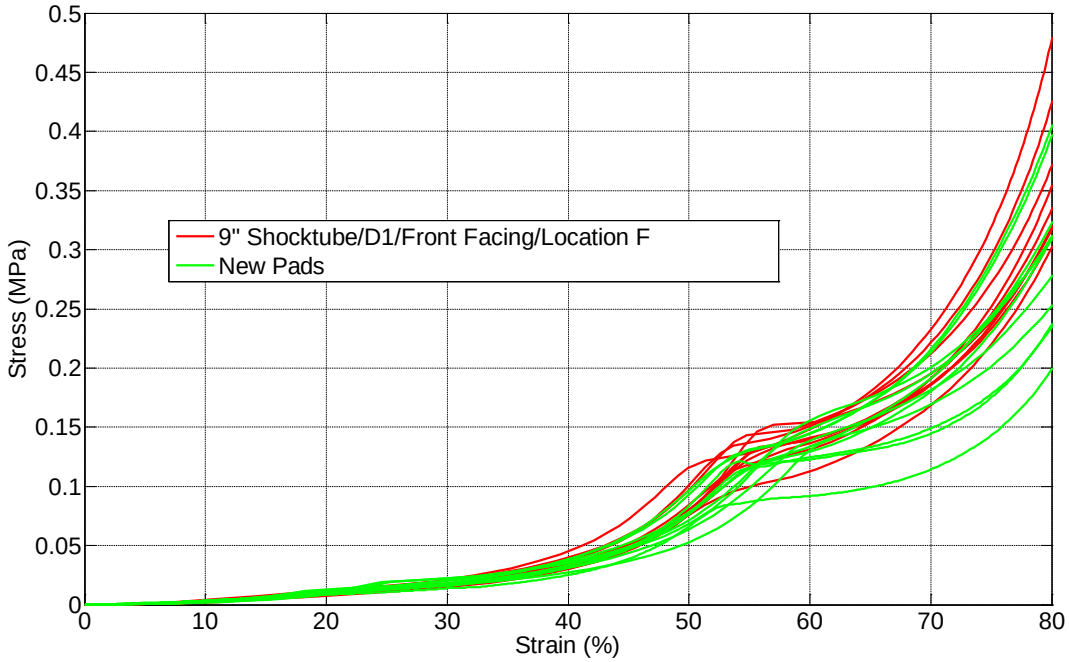

Figure A-5. Rectangular-9-inch shocktube/D1/front facing/location F vs. new pads.

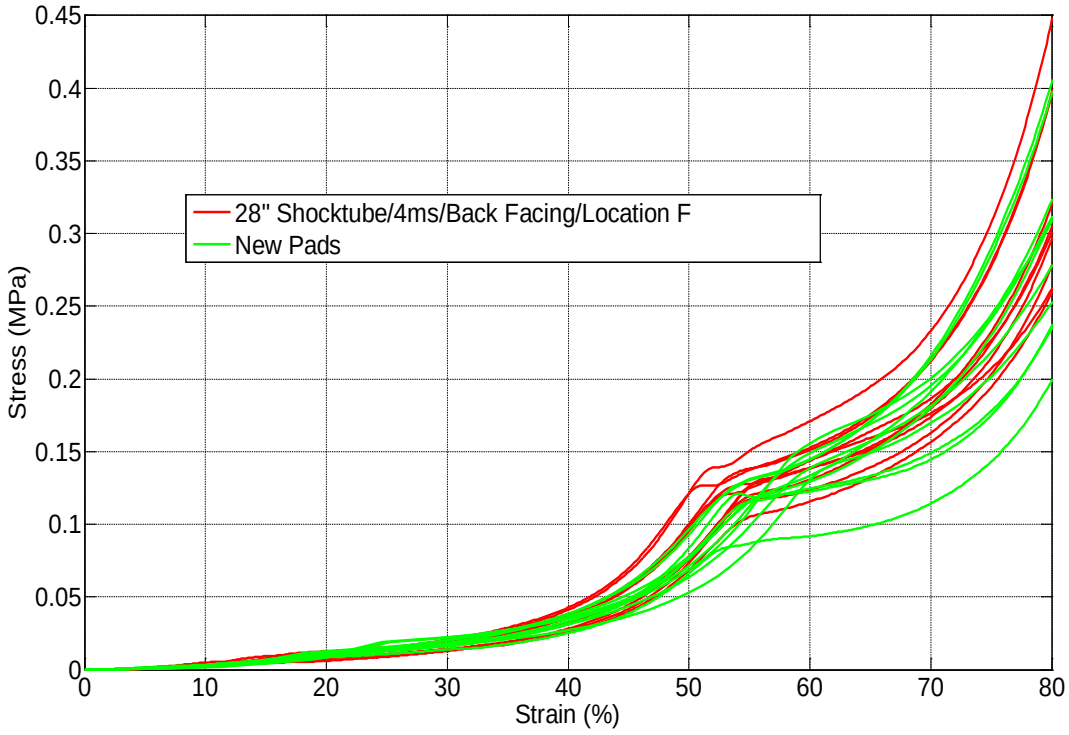

Figure A-6. Rectangular-28-inch Shocktube/4-ms/back facing/location F vs. new pads.

The results from the tests of the trapezoidal pads tested under 10 kN load cell (crosshead speed = 8 mm/s) are displayed in Figures A-7 through A-12.

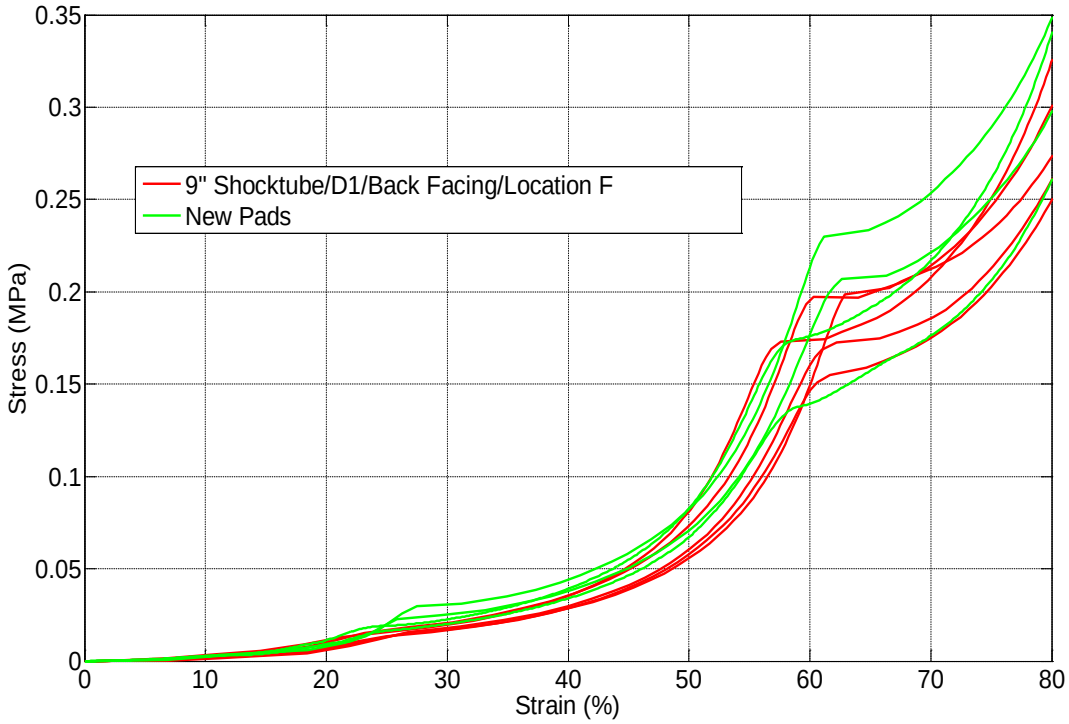

Figure A-7. Trapezoidal-9-inch shocktube/D1/back facing/location F vs. new pads.

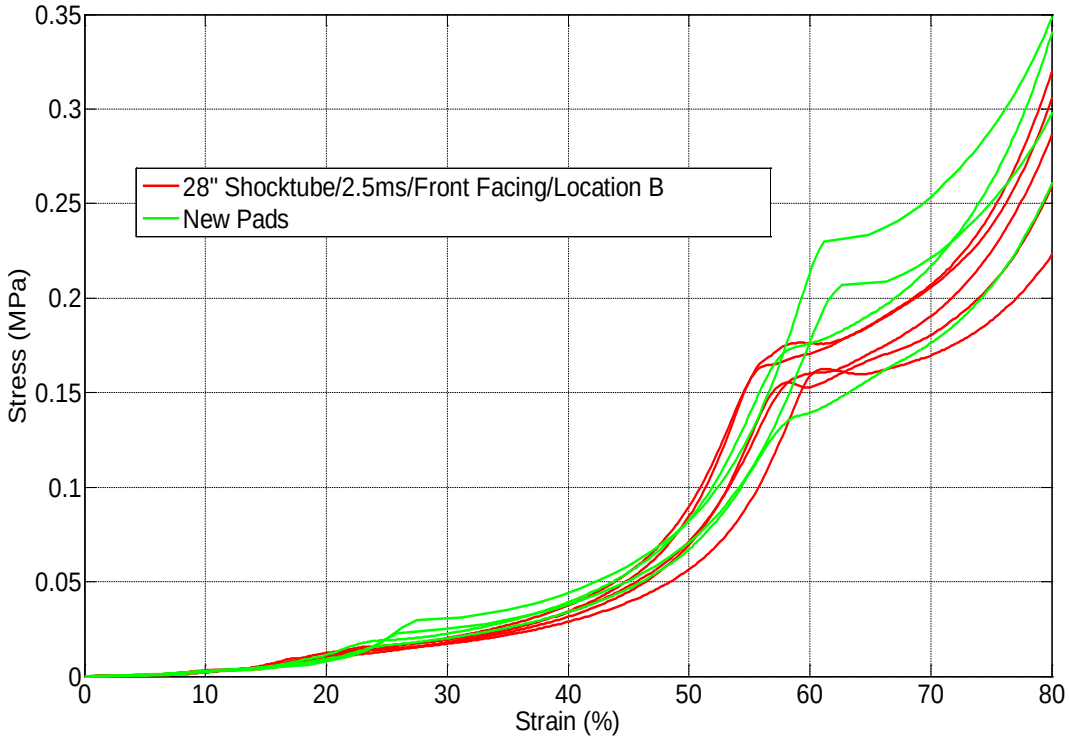

Figure A-8. Trapezoidal-28-inch shocktube/2.5-ms/front facing/location B vs. new pads.

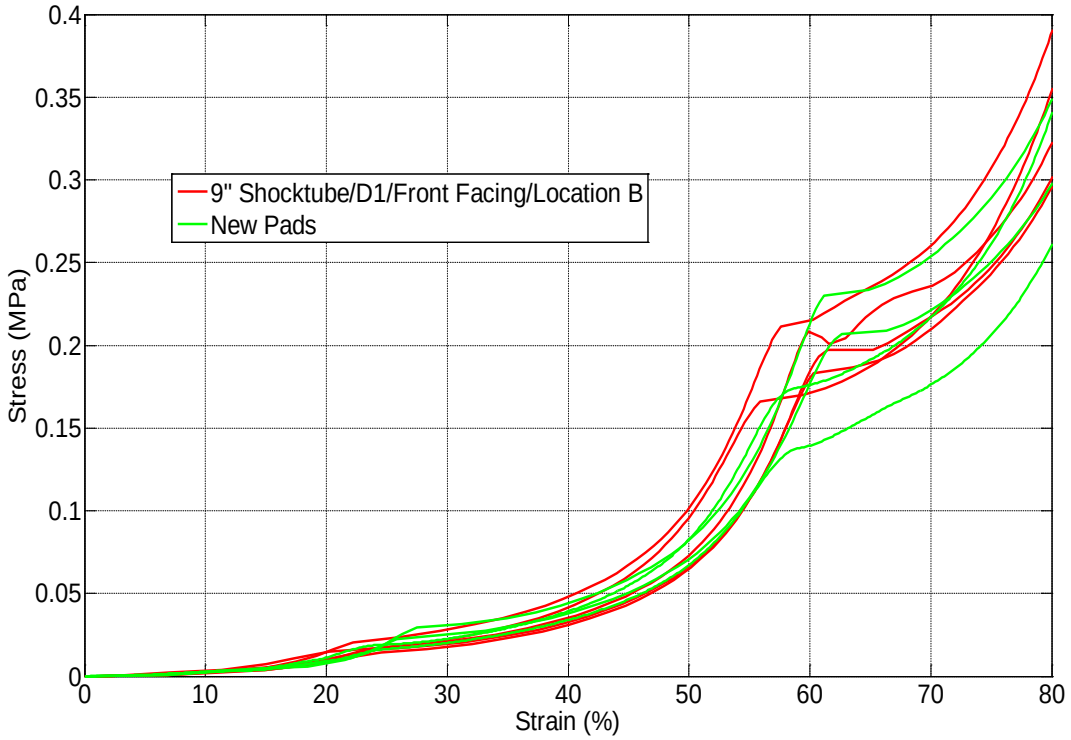

Figure A-9. Trapezoidal-9-inch shocktube/D1/front facing/location B vs. new pads.

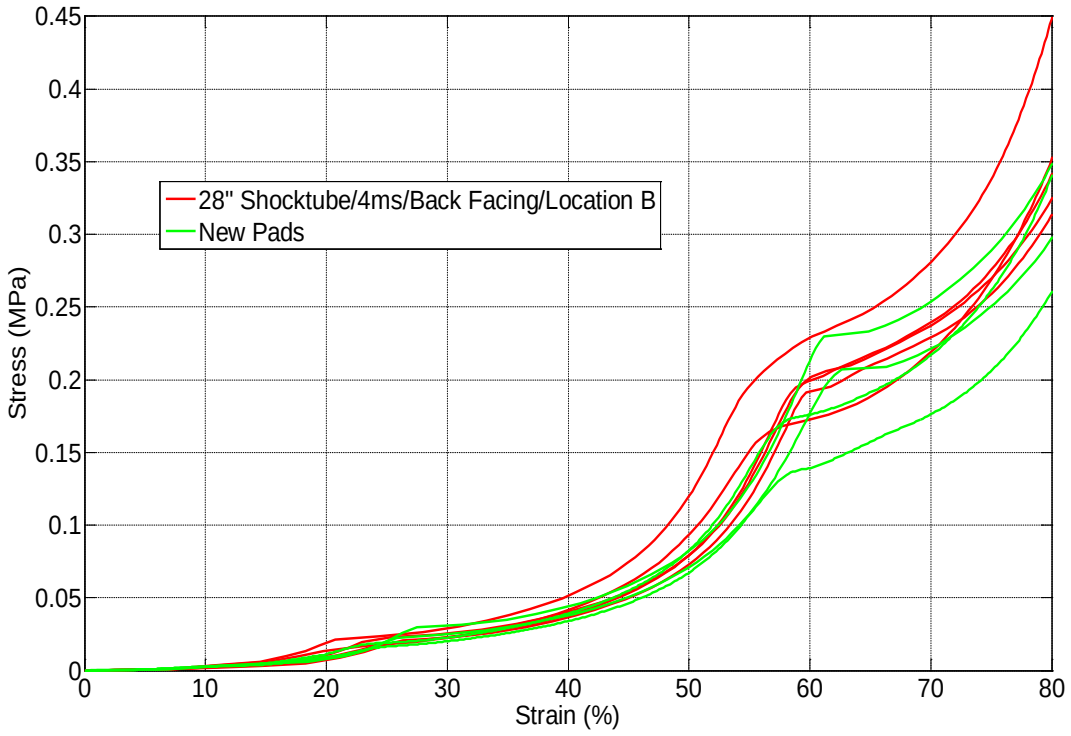

Figure A-10. Trapezoidal-28-inch shocktube/4-ms/back facing/location B vs. new pads.

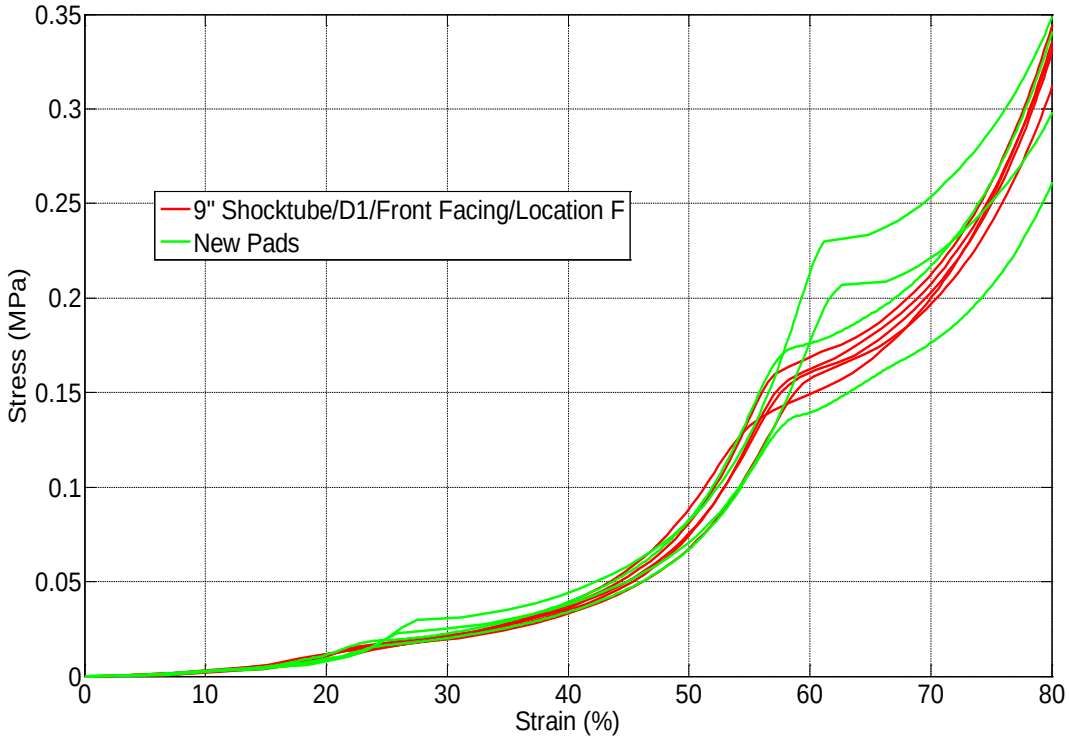

Figure A-11. Trapezoidal-9-inch shocktube/D1/front facing/location F vs. new pads.

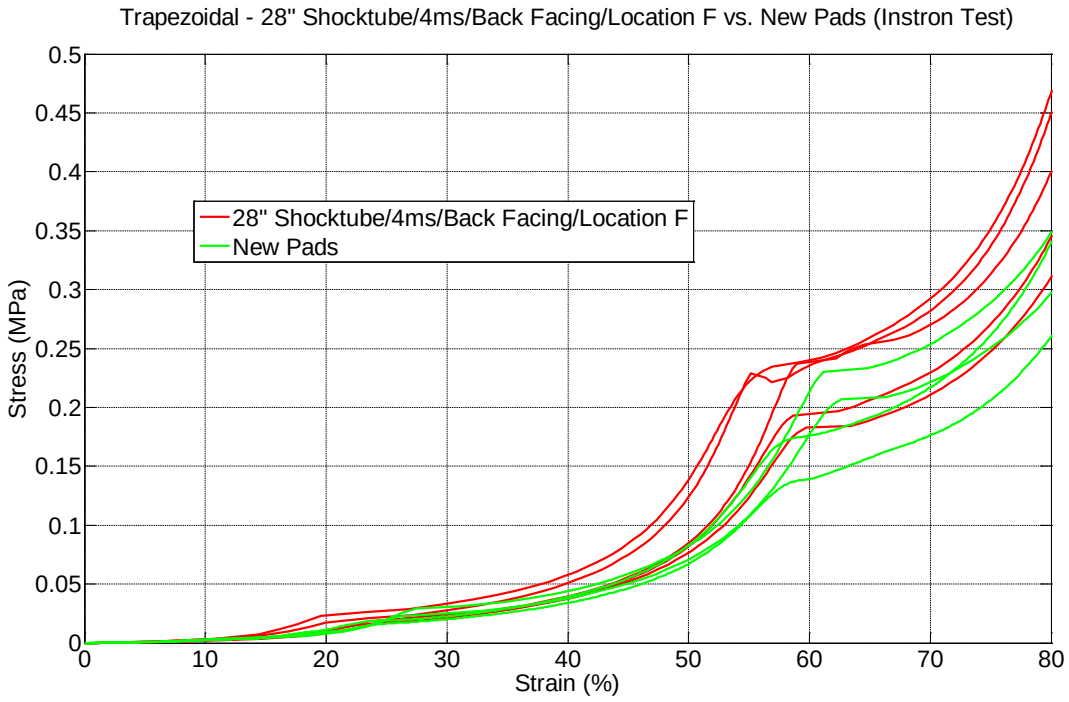

Figure A-12. Trapezoidal-28-inch shocktube/4-ms/back facing/location F vs. new pads.